

UNCLASSIFIED

AD NUMBER

AD479000

LIMITATION CHANGES

TO:

Approved for public release; distribution is unlimited.

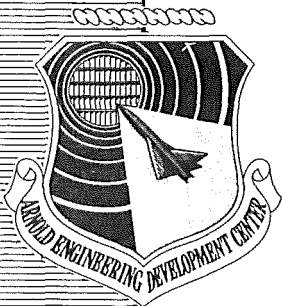
FROM:

Distribution authorized to U.S. Gov't. agencies and their contractors;
Administrative/Operational Use; MAR 1966. Other requests shall be referred to Arnold Engineering Development Center, Arnold AFB, TN.

AUTHORITY

AEDC ltr 29 Jan 1996

THIS PAGE IS UNCLASSIFIED



**AN OPEN-JET WIND TUNNEL INVESTIGATION OF
A FIXED-GEOMETRY DIFFUSER SYSTEM AT
MACH NUMBERS 3.6 AND 7.0**

**Richard F. Austin
ARO, Inc.**

March 1966

This document is subject to special export controls
and each transmittal to foreign governments or foreign
nationals may be made only with prior approval of
Arnold Engineering Development Center.

**PROPULSION WIND TUNNEL FACILITY
ARNOLD ENGINEERING DEVELOPMENT CENTER
AIR FORCE SYSTEMS COMMAND
ARNOLD AIR FORCE STATION, TENNESSEE**

NOTICES

When U. S. Government drawings specifications, or other data are used for any purpose other than a definitely related Government procurement operation, the Government thereby incurs no responsibility nor any obligation whatsoever, and the fact that the Government may have formulated, furnished, or in any way supplied the said drawings, specifications, or other data, is not to be regarded by implication or otherwise, or in any manner licensing the holder or any other person or corporation, or conveying any rights or permission to manufacture, use, or sell any patented invention that may in any way be related thereto.

Qualified users may obtain copies of this report from the Defense Documentation Center.

References to named commercial products in this report are not to be considered in any sense as an endorsement of the product by the United States Air Force or the Government.

AN OPEN-JET WIND TUNNEL INVESTIGATION OF
A FIXED-GEOMETRY DIFFUSER SYSTEM AT
MACH NUMBERS 3.6 AND 7.0

Richard F. Austin
ARO, Inc.

This document is subject to special export controls
and each transmittal to foreign governments or foreign
nationals may be made only with prior approval of
Arnold Engineering Development Center.

FOREWORD

The work reported herein was done at the request of the Arnold Engineering Development Center (AEDC), Air Force Systems Command (AFSC), under Program Element 62410034, Project 7778, Task 777805.

The results of research presented were obtained by ARO, Inc. (a subsidiary of Sverdrup and Parcel, Inc.), contract operator of AEDC, AFSC, Arnold Air Force Station, Tennessee, under Contract AF40(600)-1200. The investigation was conducted during the period of January through April 1965, in the Propulsion Wind Tunnel Facility under ARO Project No. PL2336, and the manuscript was submitted for publication on December 17, 1965.

The author expresses his appreciation to Mr. John C. Marshall for his guidance and to the Tripltee Design Criteria Staff for their significant contributions to this investigation.

This technical report has been reviewed and is approved.

G. M. Arnold
Chief, Construction Branch
Tripltee Management Office
DCS/Civil Engineering

Donald R. Eastman, Jr.
DCS/Research

ABSTRACT

A fixed-geometry second-throat diffuser system was tested in an open-jet wind tunnel at Mach numbers 3.6 and 7.0. These tests were conducted at Reynolds numbers of 1×10^6 and 2×10^5 , based on expansion nozzle exit diameter. The investigation was conducted to provide diffuser design criteria for the AEDC proposed Hypersonic True Temperature Tunnel (Tripltee). At $M_\infty = 3.6$, empty test section diffuser efficiencies of 96 percent of normal shock recovery were achieved. Under similar conditions at $M_\infty = 7.0$, efficiencies of 90 percent were obtained, thus establishing that reasonable diffuser efficiencies can be obtained at both Mach numbers with a single diffuser system. Tunnel operation was possible with conical models of up to 18-percent blockage, but diffuser efficiency was reduced by 8 to 12 percent. Tunnel flow could not be established with models in the test section. Models of 8- to 10-percent blockage would not permit establishment of tunnel flow at either $M_\infty = 3.6$ or 7.0. It was necessary to inject the models into the flow after the tunnel was started. Limited diffuser heating rate data were obtained at $M_\infty = 7.0$.

CONTENTS

	<u>Page</u>
ABSTRACT.	iii
NOMENCLATURE.	vii
I. INTRODUCTION	1
II. APPARATUS	
2.1 General Description.	1
2.2 Air Heater System	2
2.3 Expansion Nozzles	2
2.4 Diffuser System	3
2.5 Blockage Models	3
2.6 Instrumentation	4
III. EXPERIMENTAL PROCEDURE	
3.1 General	5
3.2 Data Reduction	6
3.3 Precision of Measurements	7
IV. RESULTS AND DISCUSSION	
4.1 Mach Number 3.6	8
4.2 Mach Number 7.0	11
4.3 Summary Comparisons	11
V. CONCLUSIONS	12
REFERENCES	13

ILLUSTRATIONS

Figure

1. Wind Tunnel Installation	
a. Expansion Nozzle and Test Cell.	15
b. Air Heater System	15
2. Wind Tunnel Components	16
3. Test Cell Details	17
4. Expansion Nozzle Pitot Pressure Profiles, $M_\infty = 3.6$ and 7.0	18
5. Diffuser Dimensions.	19
6. Blockage Models	20
7. Blockage Model and Model Support System Dimensions.	21

<u>Figure</u>		<u>Page</u>
8.	Blockage Model Installation in the Wind Tunnel	
	a. 2.5-in. Hemisphere-Cylinder	22
	b. 3.1-in. Cone	22
9.	Instrumentation Locations for Diffuser and Test Cell .	23
10.	Summary of Wind Tunnel Test Conditions	24
11.	Diffuser Efficiencies and Static Pressure Distributions, $M_\infty = 3.6$, 12-in. Inlet	
	a. Test Section Empty	25
	b. 2.0-in. Cone Model	26
	c. 3.1-in. Cone Model	27
12.	Diffuser Efficiencies and Static Pressure Distributions, $M_\infty = 3.6$, 10-in. Inlet	
	a. Test Section Empty	28
	b. 2.0-in. Cone Model	29
	c. 3.1-in. Cone Model	30
13.	Diffuser Efficiencies and Static Pressure Distributions, $M_\infty = 3.6$, 10-in. Inlet, Cold Flow	
	a. Test Section Empty	31
	b. 3.1-in. Cone Model	32
14.	Diffuser Efficiencies and Static Pressure Distributions, $M_\infty = 7.0$, 12-in. Inlet	
	a. Test Section Empty	33
	b. 2.0-in. Cone Model	34
	c. 2.5-in. Cone and Hemisphere-Cylinder Models	35
	d. 3.1-in. Cone Model	36
15.	Diffuser Heating Rate and Static Pressure Distributions, $M_\infty = 7.0$, 12-in. Inlet	37
16.	Model Blockage Effects on Test Cell Pressure, $M_\infty = 3.6$ and 7.0	38
17.	Model Blockage Effects on Optimum Diffuser Efficiency, $M_\infty = 3.6$ and 7.0	39
18.	Comparison of Supersonic and Hypersonic Wind Tunnel Pressure Ratios	40

NOMENCLATURE

A	Area
a	Acoustic velocity
c_p	Specific heat
D	Diameter
L	Length from nozzle throat to nozzle exit
M	Mach number, V/a
p	Static pressure
p_o	Stagnation pressure
p_o'	Pitot pressure
\dot{Q}/A	Heating rate
R	Radius of flow stream
Re	Reynolds number, $\rho_\infty V_\infty D_{NE}/\mu_\infty$
r	Radial distance from centerline of flow stream
T	Static temperature
T_o	Stagnation temperature
t	Wall thickness
V	Velocity
$\Delta T/\Delta \theta$	Temperature-time derivative
η	Diffuser efficiency, $(p_o')_{DIFF}/(p_o')_{NE} \times 100$
λ	Pressure ratio, $p_o/(p_o')_{DIFF}$
μ	Viscosity
ρ	Density

SUBSCRIPTS

c	Test cell
DIFF	Diffuser exit
EXH	Tunnel exhaust
NE	Nozzle exit
o	Stagnation conditions
∞	Free-stream conditions
*	Nozzle throat section

SECTION I INTRODUCTION

The design of a large scale, true temperature wind tunnel to be known as "Tripltee" is under study at the Arnold Engineering Development Center (AEDC). It is proposed that the exhausters systems of the Rocket Test Facility (RTF) and the Propulsion Wind Tunnel Facility (PWT) will be used to provide pressure ratio control and mass pumping for Tripltee. The characteristics of these facilities and the desired operating range for Tripltee require that efficient diffuser systems be incorporated into the wind tunnel design.

In its initial phase, Tripltee is to operate at discrete Mach numbers between $M_\infty = 3.0$ and 7.0. It is to be a large facility, and it would be highly advantageous to provide a single diffuser system that would operate efficiently over the entire Mach number range. Detailed information for design of such open-jet diffuser systems was found to be quite limited. Therefore, the present investigation was undertaken to provide additional information necessary to establish definitive design criteria for the full-scale Tripltee diffuser system.

Tests were conducted with a fixed-geometry second-throat diffuser system. The diffuser design was established with the limited information available from the literature on open-jet diffuser systems. The diffuser was tested with a series of aerodynamic models at Mach numbers 3.6 and 7.0. Axisymmetric nozzles used to generate these Mach numbers were scaled models of those proposed for the Tripltee facility.

SECTION II APPARATUS

2.1 GENERAL DESCRIPTION

The diffusers were tested in a continuous flow, nonreturn, open-jet wind tunnel specifically designed and built for this experimental investigation. The tunnel consists of a high pressure air source, air heater system, expansion nozzles, test cell, and diffuser system. Intermediate ducting connects the tunnel to the RTF exhausters system, which was used for tunnel pressure ratio control. The tunnel and its various components are shown in Figs. 1, 2, and 3.

2.2 AIR HEATER SYSTEM

Heat was added to the tunnel air by means of an electric resistance heater. The air was heated by flowing in direct contact with six elements whose temperature could be maintained at 2000°F. The heater was designed and developed in the von Kármán Gas Dynamics Facility (VKF) at AEDC. It is capable of delivering 5 lb/sec of air at temperatures approaching 2000°F. The heater is described in detail in Ref. 1. Electrical energy was continuously supplied to the heater from a d-c power supply whose output power could be closely regulated. The required input power levels to the heater were determined by monitoring the element temperatures and the air total temperature.

2.3 EXPANSION NOZZLES

The expansion nozzles used were axisymmetric, contoured nozzles designed to generate parallel flow at Mach numbers 4 and 7. The nozzle contour consists of a circular arc to the throat, an assumed cubic area distribution from the throat to the inflection point, and a potential flow characteristics solution contour from the inflection point to the nozzle exit. Calculations of the potential flow contours were carried out using the method of Cresci which is described in Ref. 2*. Viscous flow corrections were made to the contours by adding the boundary-layer displacement thicknesses calculated by the method of Sivells given in Ref. 3.

The Mach 4 nozzle was 34.48 in. long from throat to exit and had an exit diameter of 8.06 in. The Mach 7 nozzle was 48.43 in. long and had an exit diameter of 9.00 in.

The nozzle throat sections were jacketed to provide backside water cooling, and the downstream expansion sections were cooled with simple backside cooling coils. A typical arrangement of the nozzle cooling system is shown in Fig. 3.

Flows generated by these nozzles were of reasonably good quality. This is demonstrated by the pitot pressure profiles that are presented in Fig. 4. The profiles were obtained at a station 0.5 in. downstream of the nozzle exit. The final Mach numbers realized with the nozzles were 3.6 and 7.0. The boundary-layer displacement thicknesses calculated for the Mach 4 nozzle were too small. In addition, it was necessary to operate the Mach 4 nozzle at off-design conditions because of

*These calculations assume a constant specific heat ratio ($\gamma = 1.4$).

limitations imposed by other test equipment. These factors resulted in the nozzle generating a Mach number that was lower than its design Mach number.

2.4 DIFFUSER SYSTEM

The diffuser system tested was a constant area duct, 40 in. in length, fitted with a 7.5-deg conical inlet and a 3-deg conical exit. The criterion used in selecting the diffuser design was that the diffuser give good performance at both Mach 4 and 7 while operating with aerodynamic models in the tunnel. Open-jet tunnel diffuser data, available from the literature, indicated that this diffuser design would give good results at both Mach numbers. Pertinent diffuser dimensions are given in Fig. 5. The diffuser inlet was made in two sections to facilitate changes in inlet length and entrance diameter. Inlet diameters of 10 and 12 in. were available with this arrangement. The geometric open-jet length of the wind tunnel was maintained at 1.5 nozzle exit diameters throughout the entire investigation. When the diffuser inlet length and diameter were changed, the diffuser system was repositioned to maintain 1.5 nozzle diameters between the nozzle exit plane and the diffuser inlet plane. All other geometric characteristics of the diffuser were fixed.

Geometric contraction ratios provided by the diffuser were 1.25 and 1.56 for the Mach 3.6 and 7.0 systems, respectively. Contraction ratio is defined as the ratio of nozzle exit area to diffuser second-throat area. (See Ref. 4.)

The entire diffuser system was water cooled. The backside cooling system of the diffuser is shown in Fig. 3. The constant area duct downstream of the diffuser exit was spray cooled.

2.5 BLOCKAGE MODELS

The aerodynamic blockage models employed in this investigation were uncooled, 15-deg half-angle blunt cones and a hemisphere-cylinder. The models were sting mounted from a strut support system that provided for manual injection and retraction from the flow. The models are shown in Fig. 6. The blockage model dimensions are given in Fig. 7, together with those of the model support system. Installation of two of the models and the support system in the tunnel is shown in Figs. 8a and b. Figure 8a is a multiple exposure photograph which demonstrates model injection into the tunnel test section. The model nose stations were

located 1.75 in. downstream of the nozzle exit on the test section centerline.

Pitot pressure measurements were made with orifices located at the stagnation points on the models. This arrangement is shown in Fig. 7. The 1.99-in. cone model was not equipped for measuring pitot pressure.

Solid blockage values for the models and support system are tabulated below. Two blockage values are given for each model to account for the difference in size between the Mach number 3.6 and 7.0 nozzles. The blockage values represent the combined blockage of the model and support system for perfectly expanded, parallel flow from the nozzles. That portion of the strut lying outside the assumed parallel flow field was not included in the blockage values.

BLOCKAGE MODEL CHARACTERISTICS

Model Description	Model Base Area, in. ²	Model and Strut Area, in. ²		Solid Blockage, Percent of Nozzle Area	
		Mach 3.6	Mach 7	Mach 3.6	Mach 7
1.99-in. Cone	3.10	4.99	5.30	9.8	8.3
2.53-in. Cone	5.03		7.05		11.1
3.10-in. Cone	7.55	9.08	9.39	17.8	14.7
2.53-in. Hemisphere-Cylinder	5.03		7.05		11.1

NOTE: Mach 3.6 Nozzle Diameter, 8.06 in. -Area, 51.01 in.²
Mach 7 Nozzle Diameter, 9.00 in. -Area, 63.70 in.²

2.6 INSTRUMENTATION

2.6.1 System Control Instrumentation

The primary control problem encountered in operation of the wind tunnel was that of controlling the resistance air heater. Heater input power requirements were determined by monitoring the tunnel total temperature and heater element temperatures. Tunnel total temperature

was measured with four bayonet thermocouple probes installed in the tunnel stilling chamber. The probes were connected electrically in parallel to provide an average total temperature measurement. Heater element temperatures were obtained from thermocouples imbedded directly in the heater elements. These temperatures were monitored to avoid exceeding an element temperature limit of 2000°F. Wind tunnel stagnation pressure was measured with a pitot tube installed in the stilling chamber of the tunnel.

2.6.2 Diffuser and Test Cell Instrumentation

Pressures and temperatures were measured throughout the test cell and diffuser system. Locations of these measurements are shown in Fig. 9. Pressures were measured with diaphragm-type, strain-gage pressure transducers equipped with heat sinks for operation at low absolute pressures. The heat sinks prevented transducer calibration changes caused by resistance heating of the strain gage in a low pressure environment. Pitot pressure measurements were made at the two locations indicated and at the stagnation point on the blockage models. The pitot pressure probes were water cooled. All other pressure measurements were wall static pressures. The exhaust pressure measurement made at a station 240 in. downstream was used to control the tunnel exhaust system.

Temperature measurements were made with thermocouples that were installed directly into the exterior surfaces at the locations indicated in Fig. 9.

SECTION III EXPERIMENTAL PROCEDURE

3.1 GENERAL

Tests were conducted to determine diffuser pressure recovery performance at Mach numbers 3.6 and 7.0. Pressure recoveries were measured for empty test section operation of the tunnel and with blockage models present in the flow. The stagnation pressure and temperature conditions at which the tests were conducted are presented in Fig. 10, together with the test Reynolds numbers. The test conditions presented in Fig. 10 show the relationship of test Reynolds numbers to those predicted for Tripltee. Equipment limitations would not permit operation at higher test Reynolds numbers.

Diffuser pressure recoveries were measured for steady-state and transient conditions over a large range of tunnel pressure ratios. Tunnel pressure ratio, λ , is the ratio of tunnel stagnation pressure to the diffuser exit pitot pressure ($\lambda = p_o / (p_o')_{\text{DIFF}}$). The tunnel was started by lowering the tunnel exhaust pressure until supersonic flow was established throughout the test section and diffuser. Successive steady-state data were then recorded as the tunnel exhaust pressure was raised until the diffuser flow unstalled. Data were then recorded continuously as the exhaust pressure was lowered until supersonic flow was re-established or it was determined that the flow could not be restarted. When model blockage effects on diffuser performance were to be evaluated, one of the models was introduced into the flow after tunnel flow had been established. Then a data recording sequence similar to that described above for empty test section operation was carried out with the model in the tunnel test section.

In every instance, an effort was made to obtain steady-state data at the minimum pressure ratio for started flow and at the pressure ratio required for restart. This aim was not always achieved because of the inherent instability of shock systems in constant area ducts. The flow cannot be controlled as these critical pressure ratios are approached. Where steady-state data were not obtained at the critical pressure ratios, they were inferred from the transient data that were continuously recorded. Instrumentation response was sufficiently high that reliable values of the critical pressure ratios could be obtained in this manner.

3.2 DATA REDUCTION

3.2.1 Diffuser Efficiency

The diffuser efficiency used in presenting the results of this investigation is defined as

$$\eta = \frac{\text{Diffuser Exit Pressure}}{\text{Normal Shock Recovery Pressure}} \times 100 = \frac{(p_o')_{\text{DIFF}}}{(p_o')_{\text{NE}}} \times 100$$

This efficiency employs a reference normal shock recovery pressure. The reference recovery pressure was measured with a flat-faced pitot pressure probe on the centerline of the test section at an axial station 0.5 in. downstream of the nozzle exit. When the tunnel was operated with blockage models in the flow, reference recovery pressures were measured at the stagnation point on the models. These measurements were made at an axial station 1.75 in. downstream of the nozzle exit. Differences in the reference recovery pressures measured at the two stations were small and are included in the overall level of precision

quoted for diffuser efficiency. The diffuser exit pressure was also measured with a flat-faced pitot pressure probe located on the centerline of the diffuser duct.

3.2.2 Diffuser Heating Rates

Diffuser heating rates were computed from temperature measurements made on the diffuser. At $M_\infty = 7.0$, heating rates were calculated, assuming thin shell radial heat transfer in a homogeneous material, according to the following equation

$$\dot{Q}/A = \rho t c_p \frac{\Delta T}{\Delta \theta}$$

Theoretical heating rates were calculated using the equation for heat transfer in a tube with turbulent flow given in Ref. 5. Stanton numbers were computed at the diffuser inlet and exit, and a linear variation of this parameter was assumed to exist between these two stations. Diffuser exit Stanton number was calculated assuming adiabatic temperature recovery. The diffuser was divided into sections of equal length, and a heating rate was calculated for each section. The flow enthalpy was adjusted at each section to reflect the loss in energy to the diffuser wall in the previous section.

3.2.3 Test Section Flow Properties

Test section flow properties were determined from the tables and charts presented in Ref. 6. The test section Mach number, M_∞ , was determined from measurements of nozzle exit pitot pressure and tunnel stagnation pressure and temperature. These measurements were corrected for caloric imperfections and related to perfect gas conditions to permit use of the tables mentioned above. Similar corrections were made to all other test section flow properties.

3.3 PRECISION OF MEASUREMENTS

A deadweight pressure calibration apparatus was used to make periodic checks on each pressure transducer and the recording systems. The recorders were adjusted to give full-scale output for the proper pressure, and the calibrations provided the means for converting the readings into pressure data.

No effective means were available for calibration of thermocouple temperature measurements. However, the temperature measuring systems were given periodic response and circuit resistance checks to ensure proper operation.

Estimates of the precision of measurements are presented below. These estimates are based on consideration of all factors known to influence these measurements. The precision levels presented correspond to a confidence level of 95 percent.

P_o	T_o	M_∞	η	p	\dot{Q}/A
± 0.1 atm	$\pm 100^\circ\text{R}$	± 0.10	± 3 percent	± 2 torr	± 0.05 Btu/ft ² -sec

SECTION IV RESULTS AND DISCUSSION

Diffuser efficiencies and wall static pressure distributions are presented for operation with the tunnel test section empty and with a series of aerodynamic models in the flow. Diffuser heating rates are presented for one $M_\infty = 7.0$ test. The measured heating rates are compared with heating rates calculated from turbulent flow heat-transfer theory. The optimum diffuser efficiencies are summarized and compared with data from other supersonic and hypersonic wind tunnels.

Diffuser efficiencies are presented over a range of tunnel pressure ratios that includes both started and unstarted diffuser operation. When the diffuser system is started, supersonic flow exists throughout the diffuser inlet and second throat. Under these conditions the test cell pressure is independent of tunnel pressure ratio. In this region two specific flow conditions are used in presenting the data. "Flow Condition 1" exists when excessive pressure ratio is developed across the tunnel. Diffuser efficiency is low for this condition of operation. "Flow Condition 2" is reached when the tunnel is operated at near-minimum pressure ratio. At Flow Condition 2, the diffuser is operating at near-maximum efficiency. Further reduction of the tunnel pressure ratio causes the diffuser to unstart, and the test cell pressure becomes dependent upon tunnel pressure ratio. Flow through the diffuser becomes subsonic, and the test cell pressure rises to levels much higher than those associated with started diffuser operation. This condition is defined as "Flow Condition 3" in the data presentation.

4.1 MACH NUMBER 3.6

Diffuser efficiencies are presented in Fig. 11 for the diffuser with a 12-in. -diam inlet at $M_\infty = 3.6$. The results of Fig. 11a typify the operating characteristics of the diffuser system. A strong hysteresis effect is observed with changes in tunnel pressure ratio. Test cell pressure is seen to be independent of pressure ratio until the diffuser

flow unstarts. With unstarted flow, test cell pressure reaches equilibrium at a pressure more than one order of magnitude higher than that for started diffuser flow conditions. Restarting of the diffuser system occurs at efficiencies that are approximately 27 percent lower than the optimum efficiency at Flow Condition 2.

Diffuser wall pressure distributions are presented in Fig. 11a for all three flow conditions. At maximum pressure ratio, supersonic flow persists throughout the diffuser. This is manifested by small pressure gradients through the diffuser and low diffuser efficiency. Large gradients occur at near-optimum efficiency and are indicative of proper diffuser performance.

When models are injected into the test section flow, the diffuser efficiencies are reduced. Comparison of the results of Figs. 11b and c with those of Fig. 11a, for empty tunnel operation, shows that diffuser efficiency is reduced 6 to 8 percent when the models are present in the flow. The diffuser wall pressure distributions show that the models alter the flow by delaying the compression process in the diffuser throat. This causes the flow to negotiate the final shock system at higher Mach numbers and results in reduced efficiency.

The diffuser system could not be restarted with any of the models in the test section. The data of Figs. 11b and c show that, when the diffuser could not be restarted, the test cell pressures remained many times higher than when the diffuser was started.

At $M_\infty = 3.6$, difficulty was encountered with empty test section starting of the 12-in. inlet diffuser configuration. Several attempts were usually necessary to effect started flow conditions.

Results obtained with the 10-in. -diam inlet configuration are presented in Fig. 12. Comparison of these results with those obtained with the 12-in. inlet shows significant gains in diffuser efficiency. At Flow Condition 2, efficiencies obtained with models are 2 to 5 percent higher than those obtained with the 12-in. inlet system. Similar gains were realized in empty test section performance.

Empty test section starting difficulties were not encountered with the 10-in. -diam inlet diffuser configuration. However, the diffuser still could not be restarted with models in the flow.

The effective open-jet length of the tunnel was varied during this investigation. The effective open-jet length is the distance from the nozzle exit to the point of flow impingement inside the diffuser inlet. Reduction of the inlet length, while maintaining a constant geometric

open-jet length, moves the point of flow impingement in the inlet closer to the nozzle exit plane. This reduces the effective open-jet length.

The shorter effective tunnel open-jet length provided by the 10-in. inlet reduced blockage model influence on the diffuser flow compression process. Contrasting the pressure distributions of Figs. 11b and c with those presented in Figs. 12b and c illustrates this point. The pressure distributions of Figs. 12b and c depict a smooth, continuous flow compression that is indicative of proper diffuser operation. This is ultimately reflected by the improved efficiencies obtained with the 10-in. inlet diffuser configuration.

Diffuser data were obtained at $M_\infty = 3.6$ at two different reservoir conditions with the 10-in. inlet configuration. A comparison of the two test conditions is shown in Fig. 10. The two conditions were run at essentially the same Reynolds number ($Re \approx 1 \times 10^6$) but with a large variation in tunnel stagnation temperature. Comparison of the results of Figs. 13a and b with those of Figs. 12a and c shows that diffuser efficiency and general operating characteristics are not appreciably altered by such changes in tunnel stagnation temperature. Similar results were obtained from the investigation reported in Ref. 7 which show that diffuser performance is not significantly affected by large changes in stagnation temperature.

At Flow Condition 1 in Fig. 13b, the flow is supersonic throughout the diffuser, and it is likely that flow separation has occurred in the divergent portion. This condition indicates that the diffuser flow has not been properly decelerated and gives rise to erroneously high diffuser efficiencies. The data at Flow Condition 1 are only presented to demonstrate the operating characteristics of the diffuser system at large tunnel pressure ratios.

Results presented thus far show that empty test section diffuser efficiencies up to 96 percent of normal shock recovery can be obtained at Mach number $M_\infty = 3.6$ and Reynolds number 1×10^6 . Diffuser efficiency is reduced 8 percent when a moderately blunt cone model of 18-percent (3.1-in.-diam) solid blockage is present in the flow. The diffuser could not be started with models in the flow. Rapid transient starts were attempted with models, but started flow could not be effected even under these conditions. The starting problem encountered at $M_\infty = 3.6$ with the 12-in. inlet diffuser system indicates that open-jet length and diffuser inlet geometry are critical factors in diffuser design. This is confirmed by the conclusions reached in Ref. 7.

4.2 MACH NUMBER 7.0

The 12-in. -diam inlet diffuser configuration was tested at $M_\infty = 7.0$. Results from these tests are presented in Fig. 14. The maximum empty test section efficiency from Fig. 14a is 90 percent. Fifteen-percent blockage of the test section with the 3.1-in. cone model reduced the diffuser efficiency to 78 percent. This is shown in Fig. 14d. Diffuser efficiencies obtained with two smaller cone models are presented in Figs. 14b and c. The hemisphere-cylinder model results presented in Fig. 14c are with the diffuser unstated. Started flow could not be maintained when the hemisphere-cylinder model was injected into the test section flow. The diffuser could not be started with any of the models in the test section. It was always necessary to inject the models after flow was established. ✓

Diffuser pressure distributions presented in Fig. 14 show that a considerable portion of the compression process takes place downstream of the diffuser throat. These results indicate that the throat section was too short to provide adequate shock compression length. Comparison of the pressure distributions of Fig. 11 with those of Fig. 14 shows the effect of throat length on the compression process. At $M_\infty = 3.6$ (Fig. 11) nearly all the flow compression takes place in the diffuser throat, indicating that the throat length was properly sized for this test condition. These results indicate that higher efficiencies could be obtained at $M_\infty = 7.0$ with a longer diffuser throat. ✓

Measured and theoretical diffuser heating rates at $M_\infty = 7.0$ are presented in Fig. 15. Heating rates were obtained by shutting off the diffuser cooling system and recording time histories of the diffuser temperatures. The measured heating rates were obtained for empty test section operation of the tunnel, at near-optimum diffuser efficiency. The diffuser wall pressure distribution presented was obtained at the same flow condition. The measured and theoretical results agree very well in the inlet and throat portion of the diffuser. Downstream of the throat, the results do not agree, which may indicate the presence of flow separation in this portion of the diffuser. The limited results presented indicate that the simple theoretical method, previously described, is adequate for predicting diffuser heat rates in these flow regimes.

4.3 SUMMARY COMPARISONS

The data presented in Fig. 16 illustrate the effect of model size and diffuser inlet geometry on the test cell pressure. The test cell pressures were obtained at Flow Condition 2, and the free-stream static pressure

was assumed to be equal to the nozzle exit static pressure with no model in the airstream. The nozzle exit pressure was unaffected by the addition of models except for the largest cone model at $M_\infty = 3.6$ with the 12-in. inlet. For this case, the nozzle exit pressure was increased approximately 30 percent. At $M_\infty = 3.6$, the 10-in.-diam inlet configuration shows a marked improvement in pumping effectiveness over the 12-in. inlet.

A summary of optimum diffuser efficiencies is presented in Fig. 17. These results illustrate the effect of model size and diffuser inlet geometry on diffuser performance. The optimum efficiency corresponds to the maximum diffuser pressure for which the diffuser flow remains started. For some of the configurations, the data at Flow Condition 2 correspond to the optimum efficiency. Where steady-state data were not obtained at the optimum efficiency, the curves of test cell pressure versus diffuser efficiency were faired between Flow Conditions 2 and 3 on the basis of the transient pressure data obtained. The optimum efficiencies for these cases were obtained from the faired curves and are indicated in Fig. 17 by the flagged symbols.

Tunnel pressure ratios obtained during this investigation are presented in Fig. 18 and are compared with similar data collected in other supersonic and hypersonic wind tunnels. The running pressure ratios with models were obtained with the 3.1-in. cone model. All starting pressure ratios were determined under empty test section conditions. These results show that pressure ratios obtained during this investigation are comparable to those obtained in other supersonic and hypersonic wind tunnels.

SECTION V CONCLUSIONS

Open-jet wind tunnel tests of a given fixed-geometry second-throat diffuser system at Mach numbers 3.6 and 7.0 lead to the following conclusions:

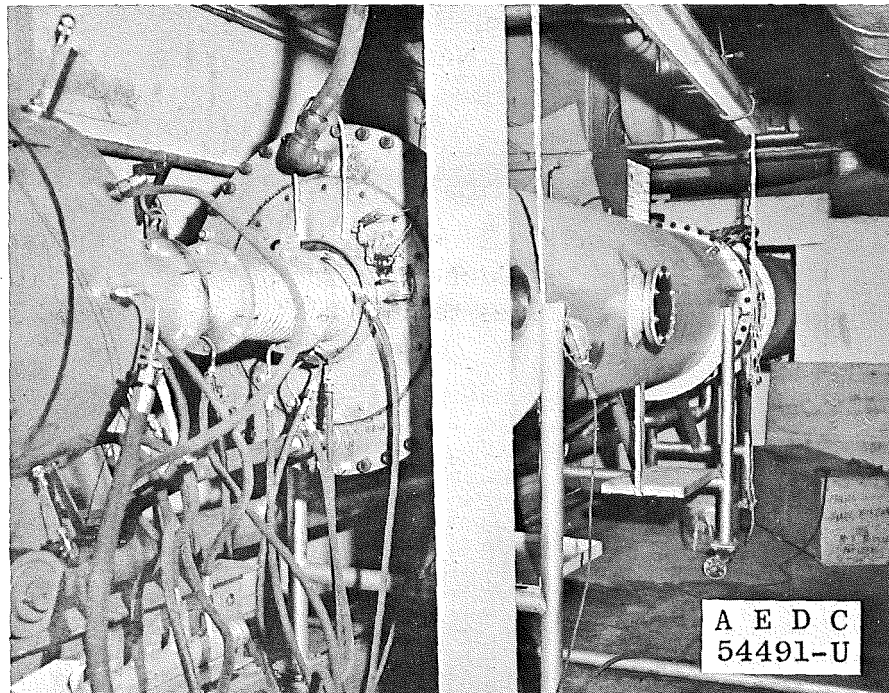
1. Empty test section diffuser efficiencies of 96-percent normal shock recovery can be achieved at $M_\infty = 3.6$ and Reynolds number of 1×10^6 .
2. At $M_\infty = 3.6$, a moderately blunt cone model of 18-percent solid blockage reduces diffuser efficiency to 88 percent of normal shock recovery.

3. Empty test section diffuser efficiencies of 90-percent normal shock recovery can be achieved at $M_\infty = 7.0$ and Reynolds number of 2×10^5 .
4. At $M_\infty = 7.0$, a moderately blunt cone model of 15-percent solid blockage reduces diffuser efficiency to 78 percent of normal shock recovery.
5. Conclusions 1 through 4 above establish that reasonably good diffuser performance can be achieved at both Mach 4 and 7 with a single diffuser configuration.
6. Diffuser flow could not be established at $M_\infty = 3.6$ or 7.0 with models in the test section. Proper diffuser operation could only be achieved by injecting the models into the test section after diffuser flow had been established.
7. Diffuser efficiency is not significantly affected by large changes in tunnel stagnation temperature.
8. Diffuser operation and performance is critically influenced by the effective open-jet length of the wind tunnel and the inlet geometry of the diffuser.
9. Limited diffuser heating rate data indicate that simple theoretical turbulent flow heat-transfer predictions are adequate for diffuser design purposes.

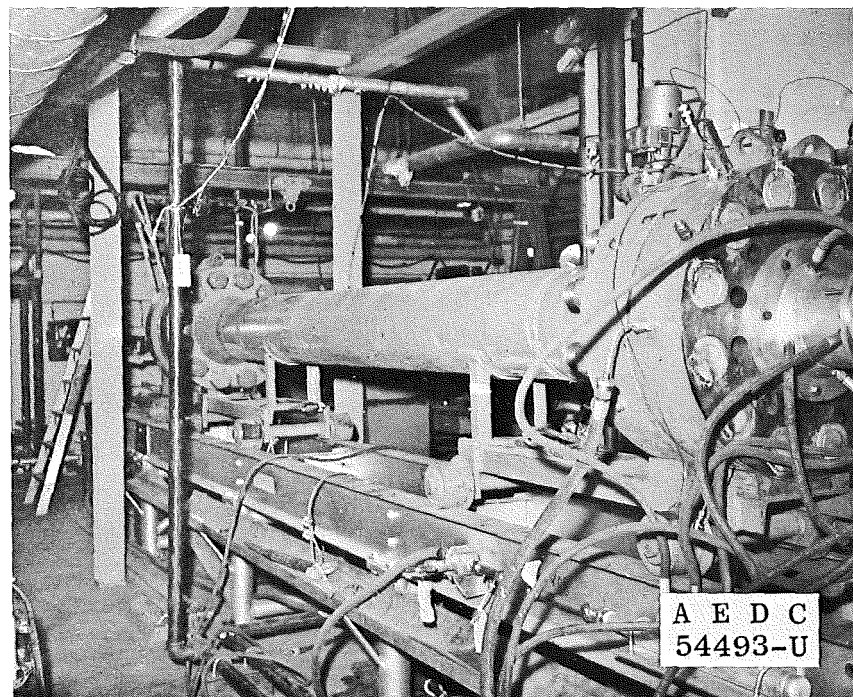
REFERENCES

1. Daniels, H. C. and Crawford, H. E. "Development and Preliminary Design of a 2000°F Air Heater." AEDC-TN-61-118, November 1961.
2. Cresci, R. J. "Tabulation of Coordinates for Hypersonic Axisymmetric Nozzles, Part I: Analysis and Coordinates for Test Section Mach Numbers of 8, 12, and 20." WADC-TN-58-300 (AD204213), October 1958.
3. Sivells, J. C. and Payne, R. G. "A Method of Calculating Turbulent-Boundary-Layer Growth at Hypersonic Mach Numbers." AEDC-TR-59-3 (AD208774), February 1959.
4. Liepmann, H. W. and Roshko, A. Elements of Gas Dynamics. John Wiley and Sons, Inc., New York, N. Y., Chapters 5 and 6, 1957.

5. Eckert, E. R. G. and Drake, R. M., Jr. Heat and Mass Transfer. McGraw-Hill Company, New York, N. Y., Section 8-2, p. 206. (Second Edition)
6. Ames Research Staff. "Equations, Tables, and Charts for Compressible Flow." NACA Report 1135, 1953.
7. Midden, R. E. and Cocke, B. W., Jr. "Diffuser Performance of a Mach 6 Open-Jet Tunnel and Model-Blockage Effects at Stagnation Temperatures to 3600°F." NASA TN D-2384, July 1964.



a. Expansion Nozzle and Test Cell



b. Air Heater System

Fig. 1 Wind Tunnel Installation

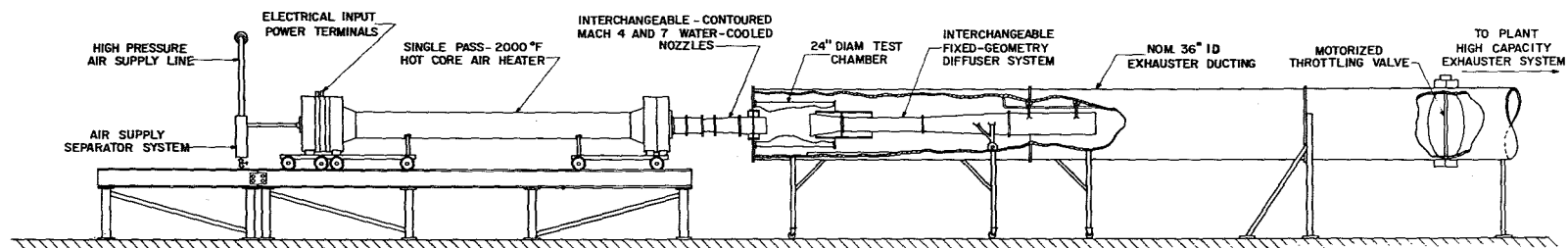


Fig. 2 Wind Tunnel Components

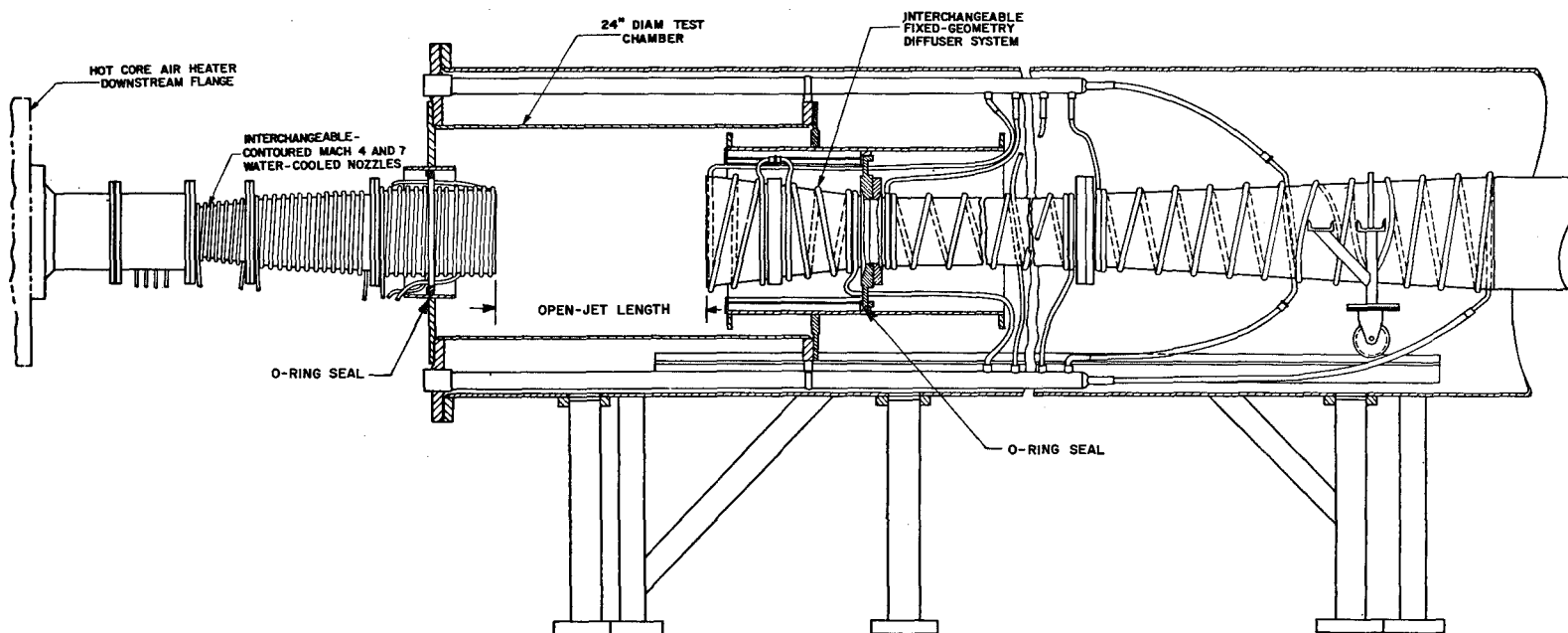


Fig. 3 Test Cell Details

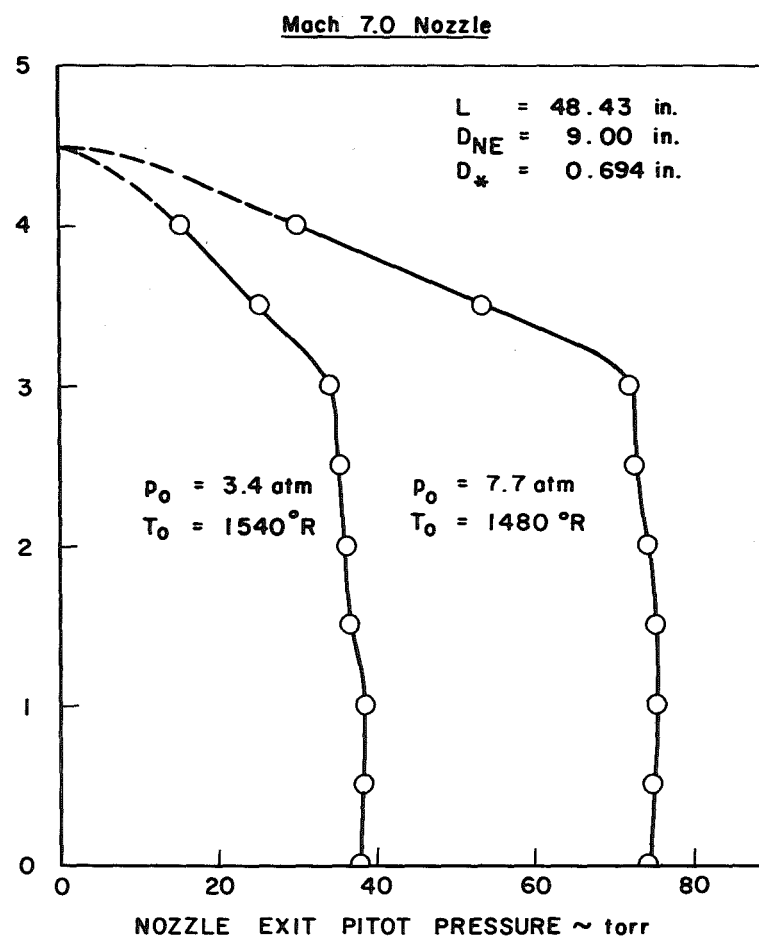
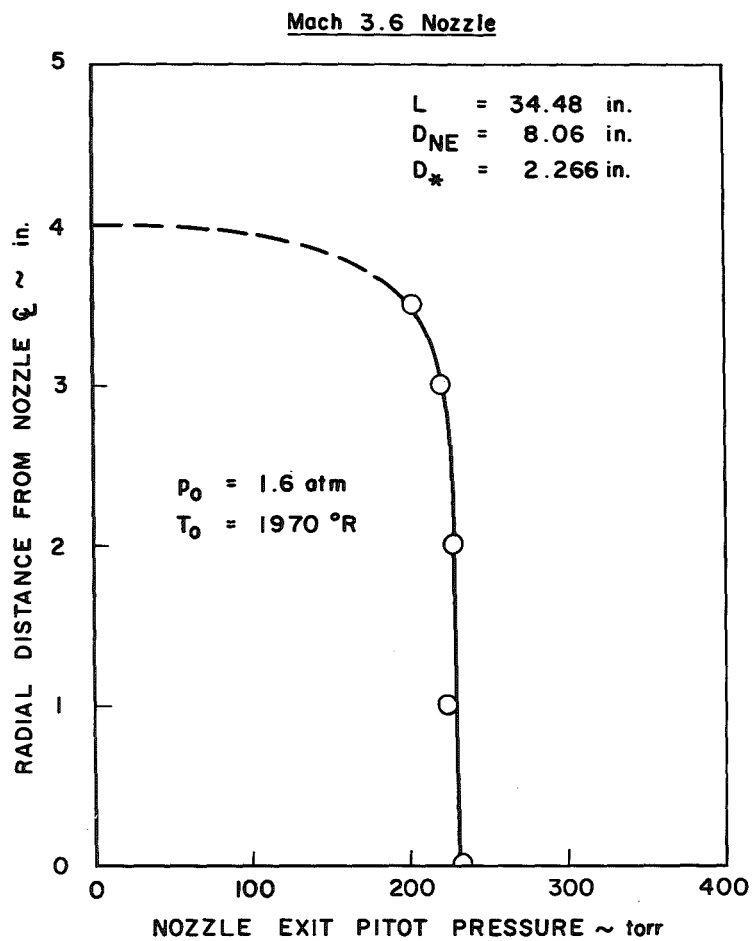
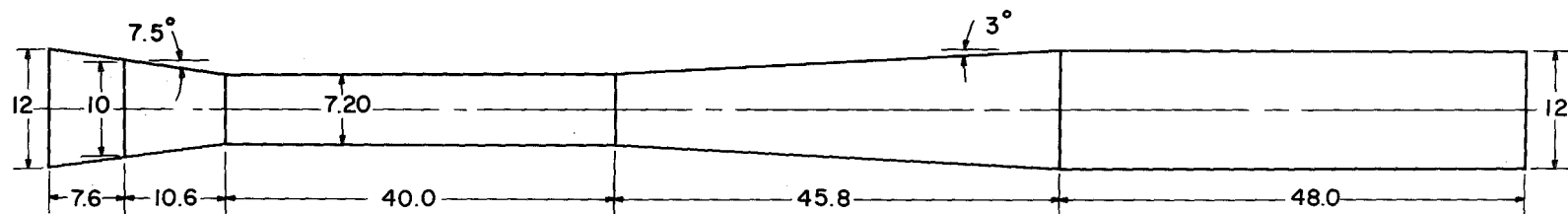


Fig. 4 Expansion Nozzle Pitot Pressure Profiles, $M_\infty = 3.6$ and 7.0



NOTE: All dimensions in inches

Fig. 5 Diffuser Dimensions

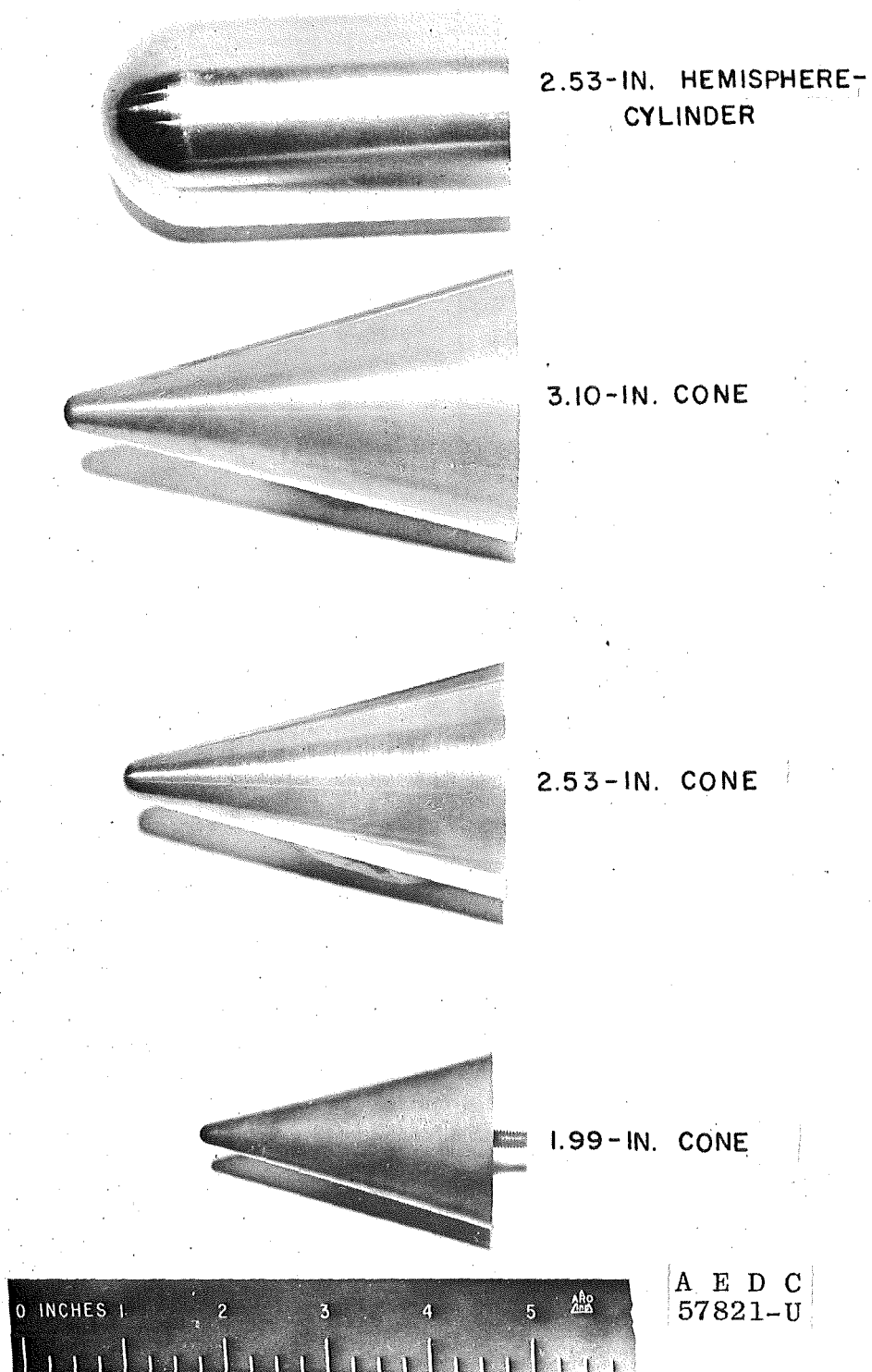


Fig. 6 Blockage Models

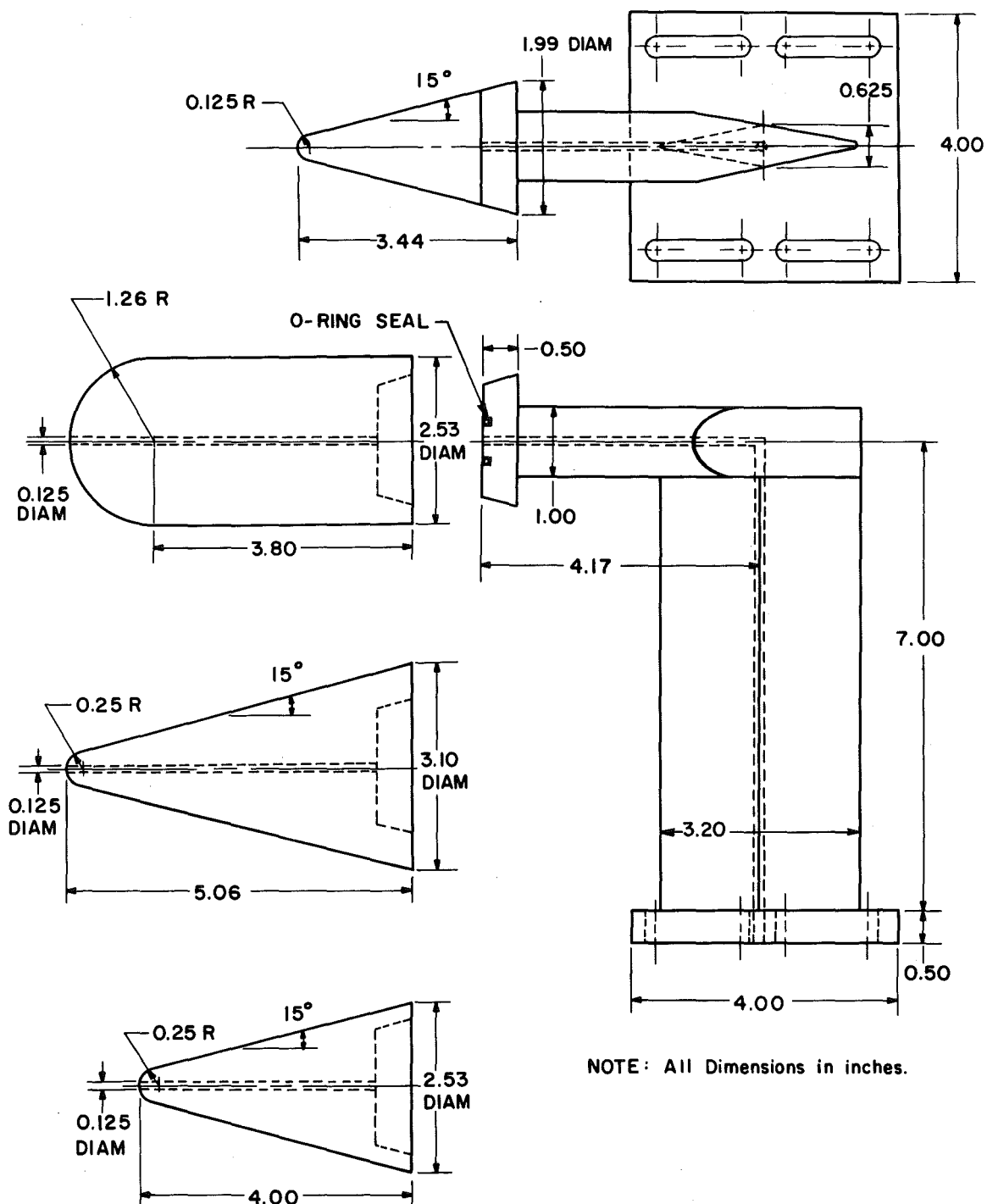
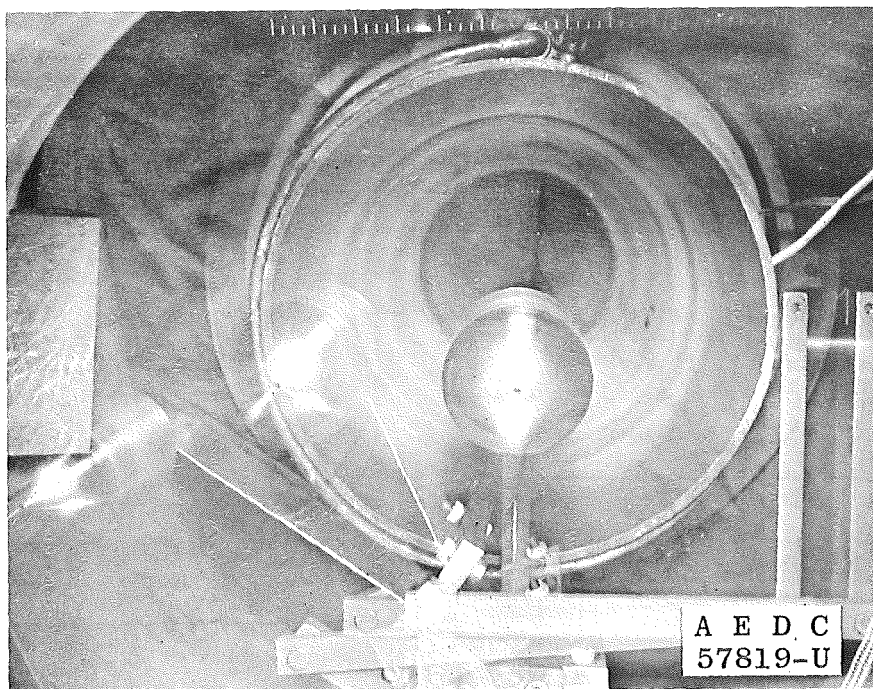
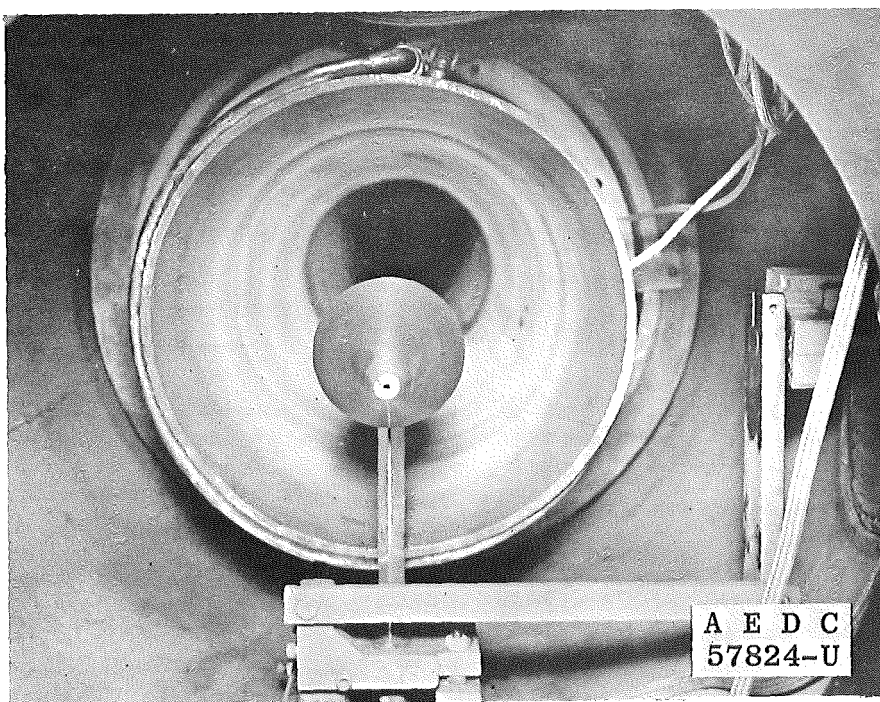


Fig. 7 Blockage Model and Model Support System Dimensions



a. 2.5-in. Hemisphere-Cylinder



b. 3.1-in. Cone

Fig. 8 Blockage Model Installation in the Wind Tunnel

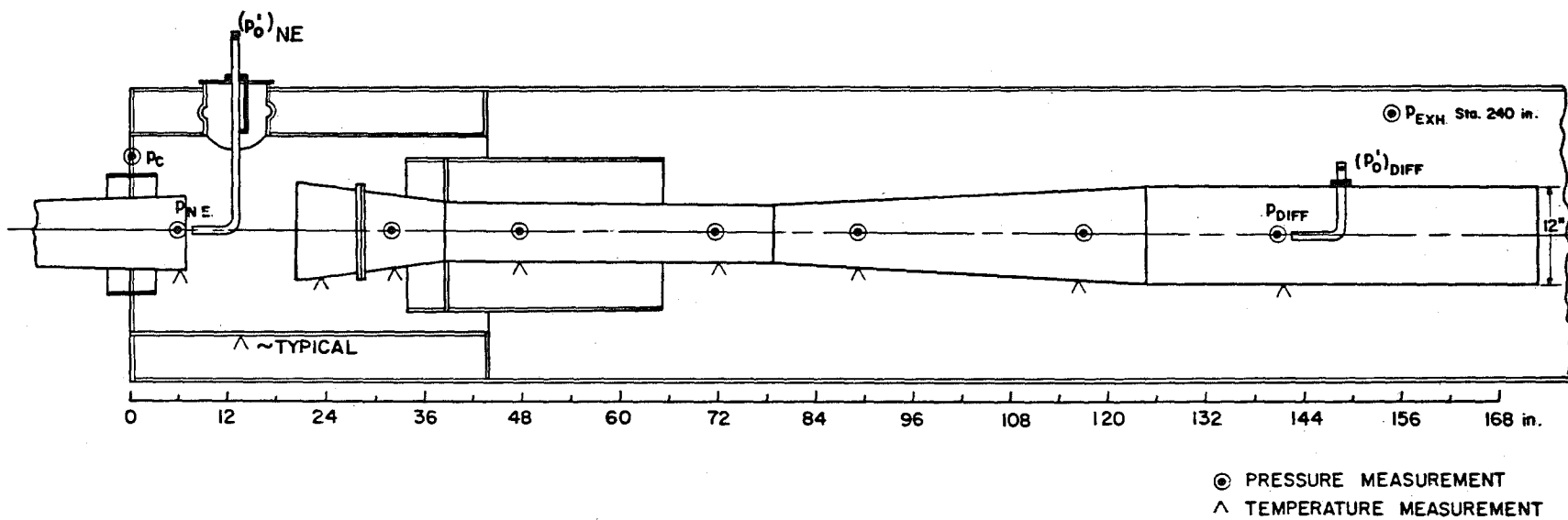


Fig. 9 Instrumentation Locations for Diffuser and Test Cell

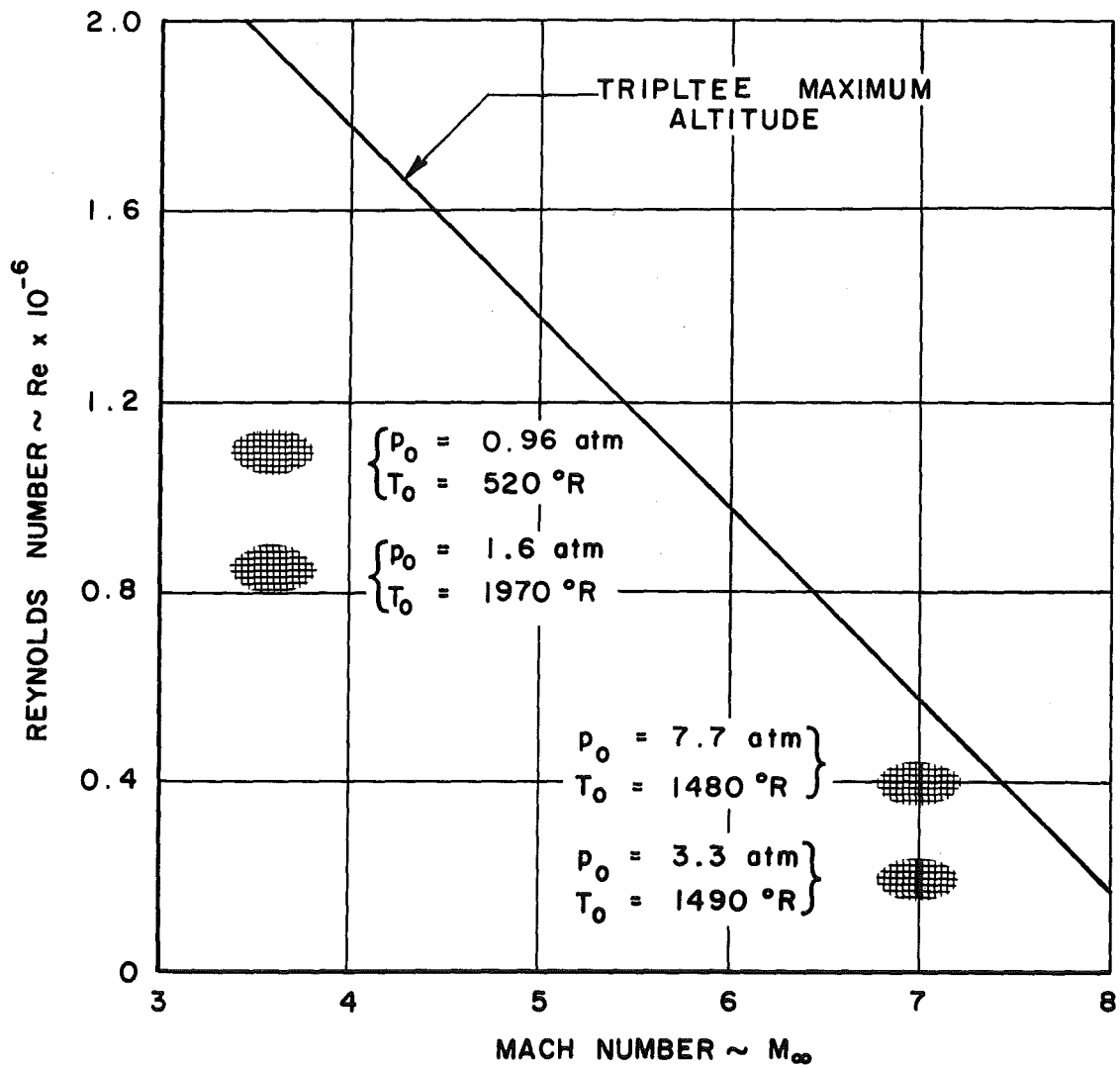
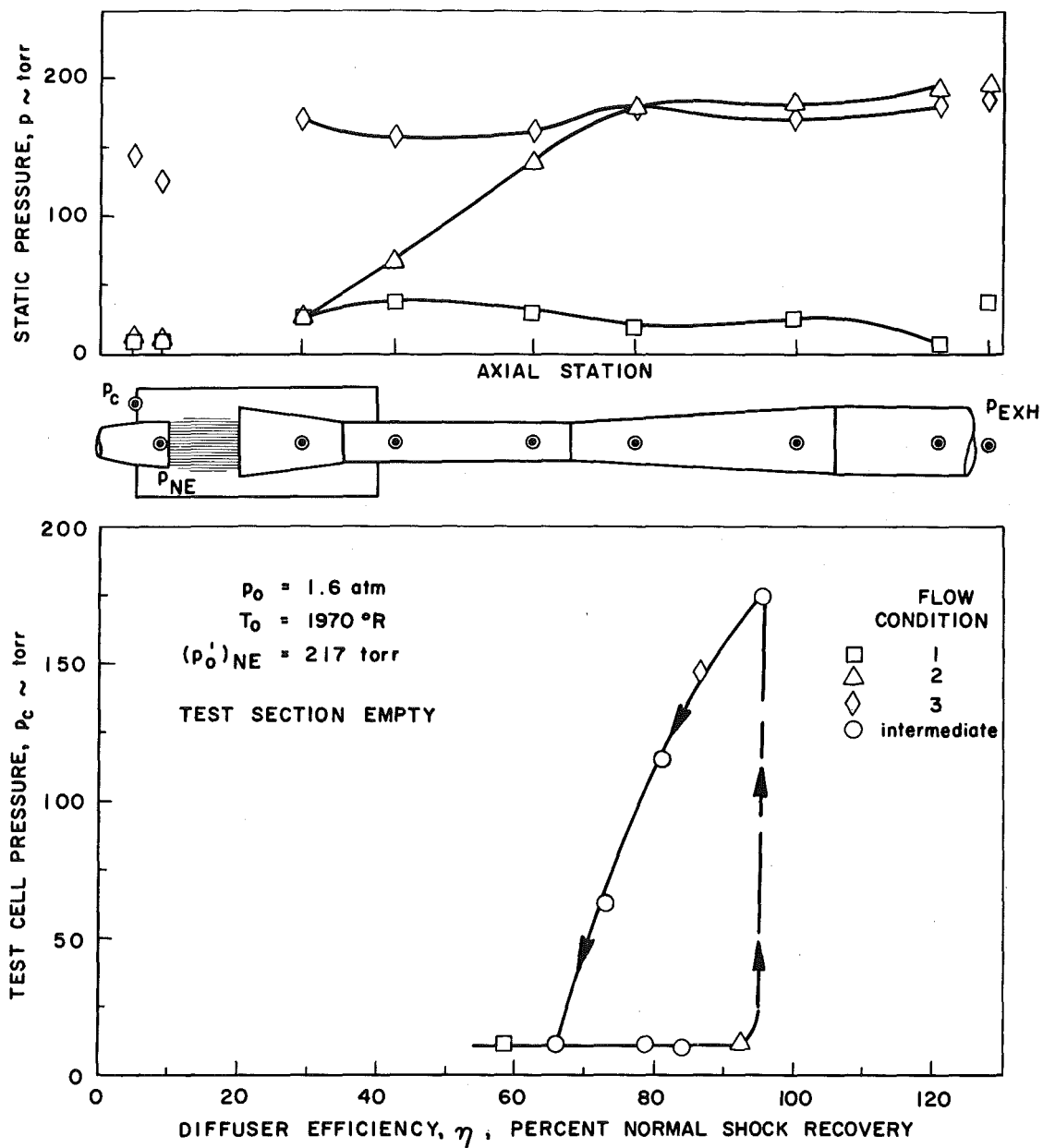
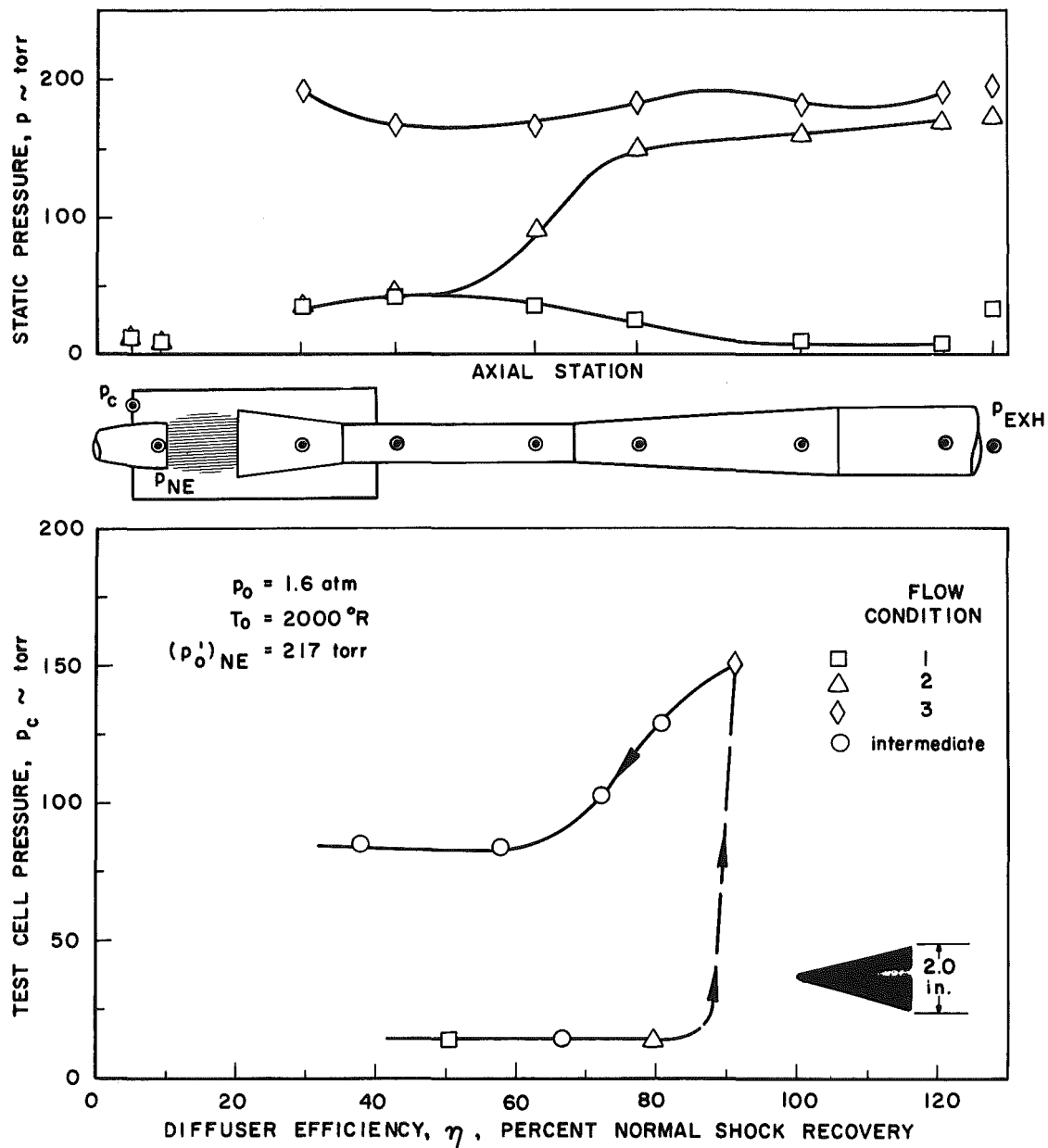


Fig. 10 Summary of Wind Tunnel Test Conditions



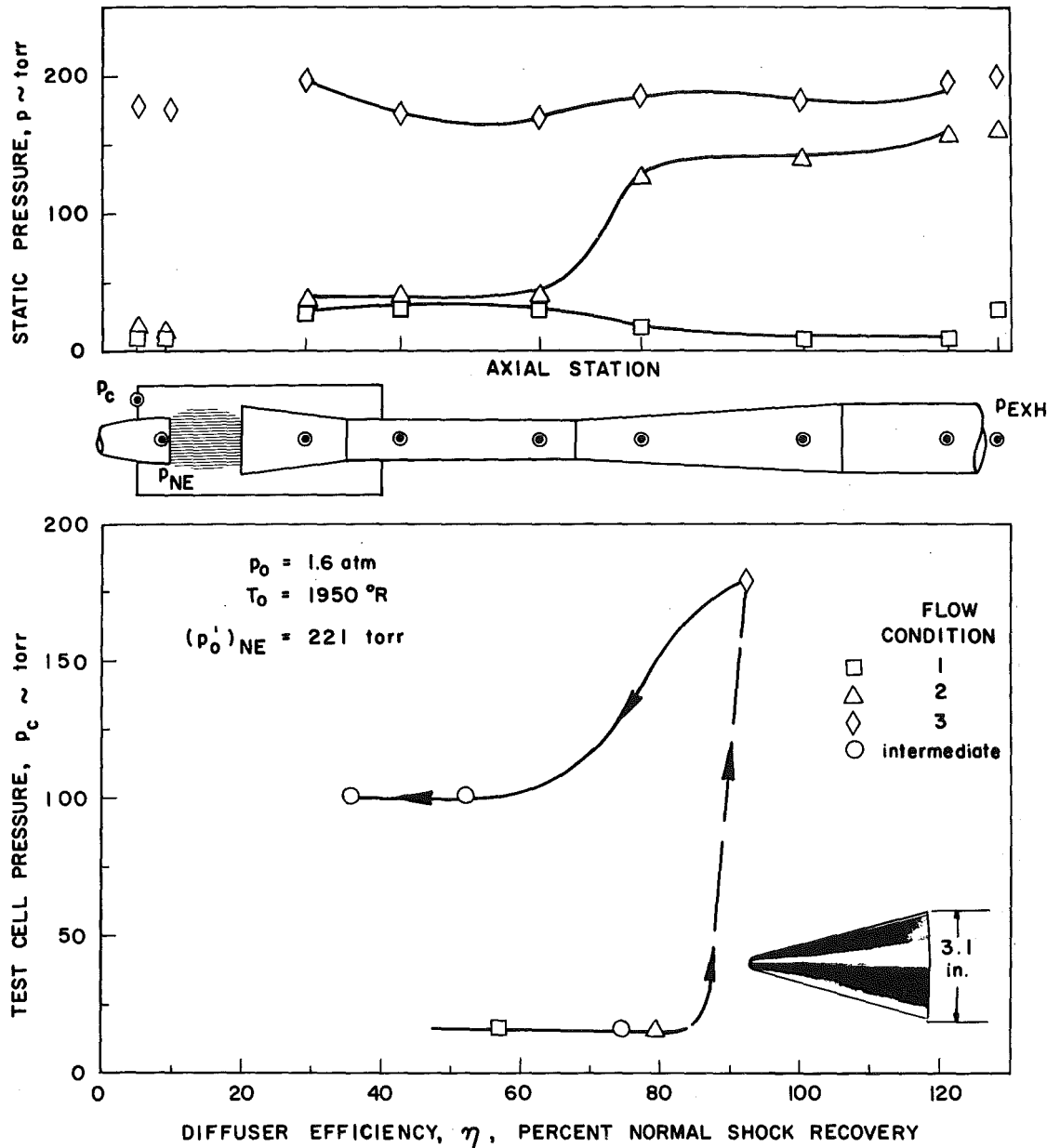
a. Test Section Empty

Fig. 11 Diffuser Efficiencies and Static Pressure Distributions,
 $M_\infty = 3.6$, 12-in. Inlet



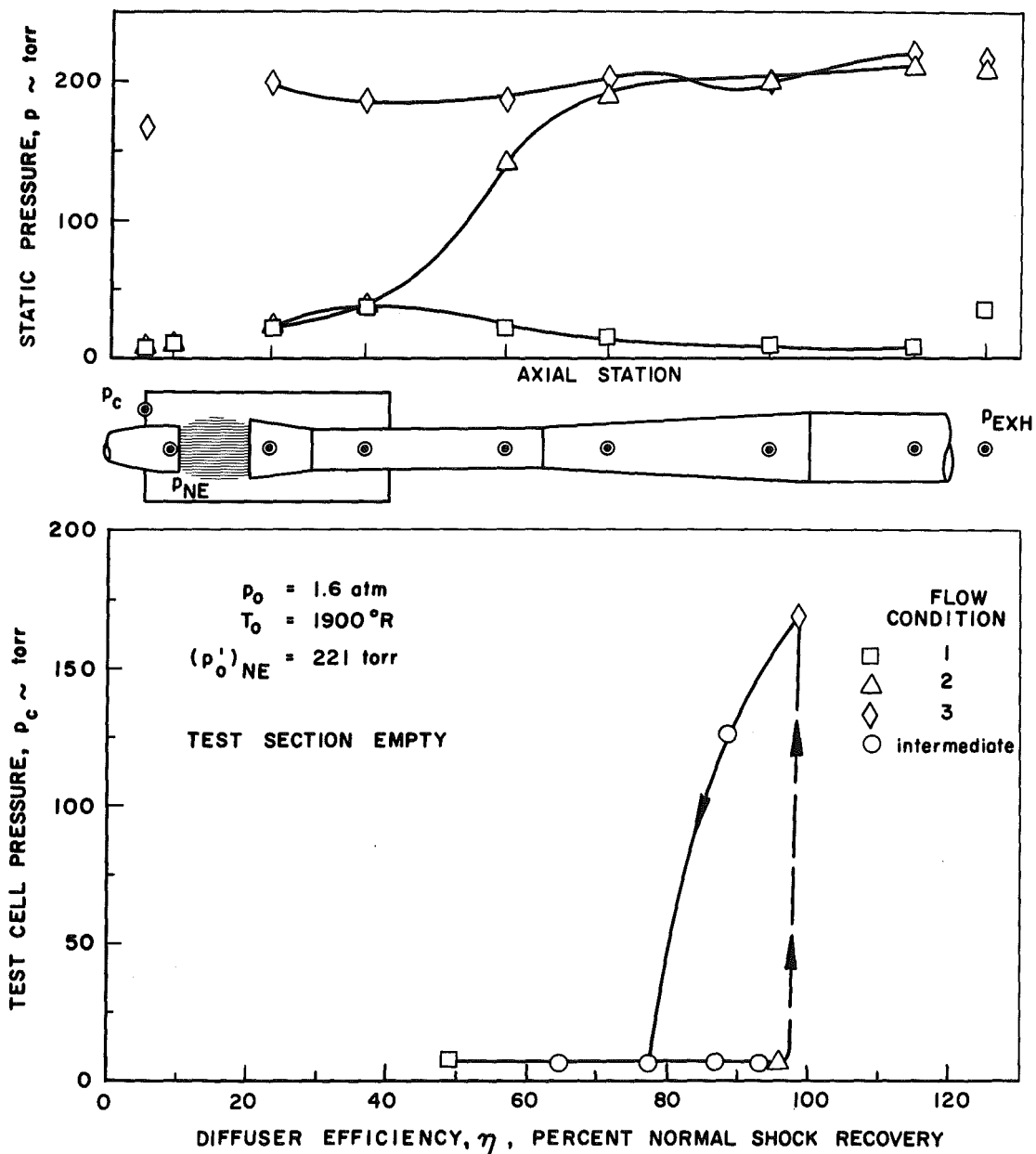
b. 2.0-in. Cone Model

Fig. 11 Continued



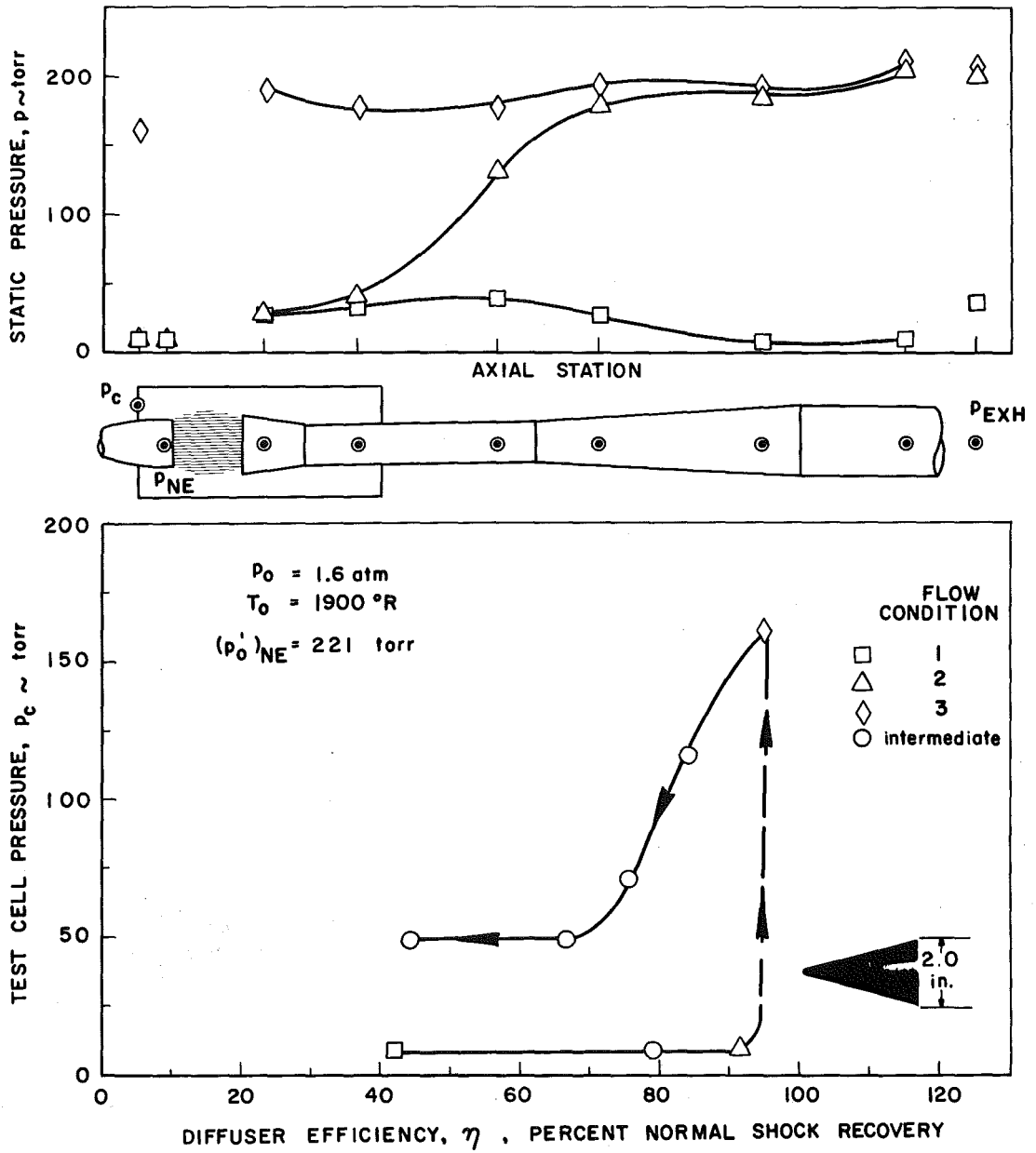
c. 3.1-in. Cone Model

Fig. 11 Concluded



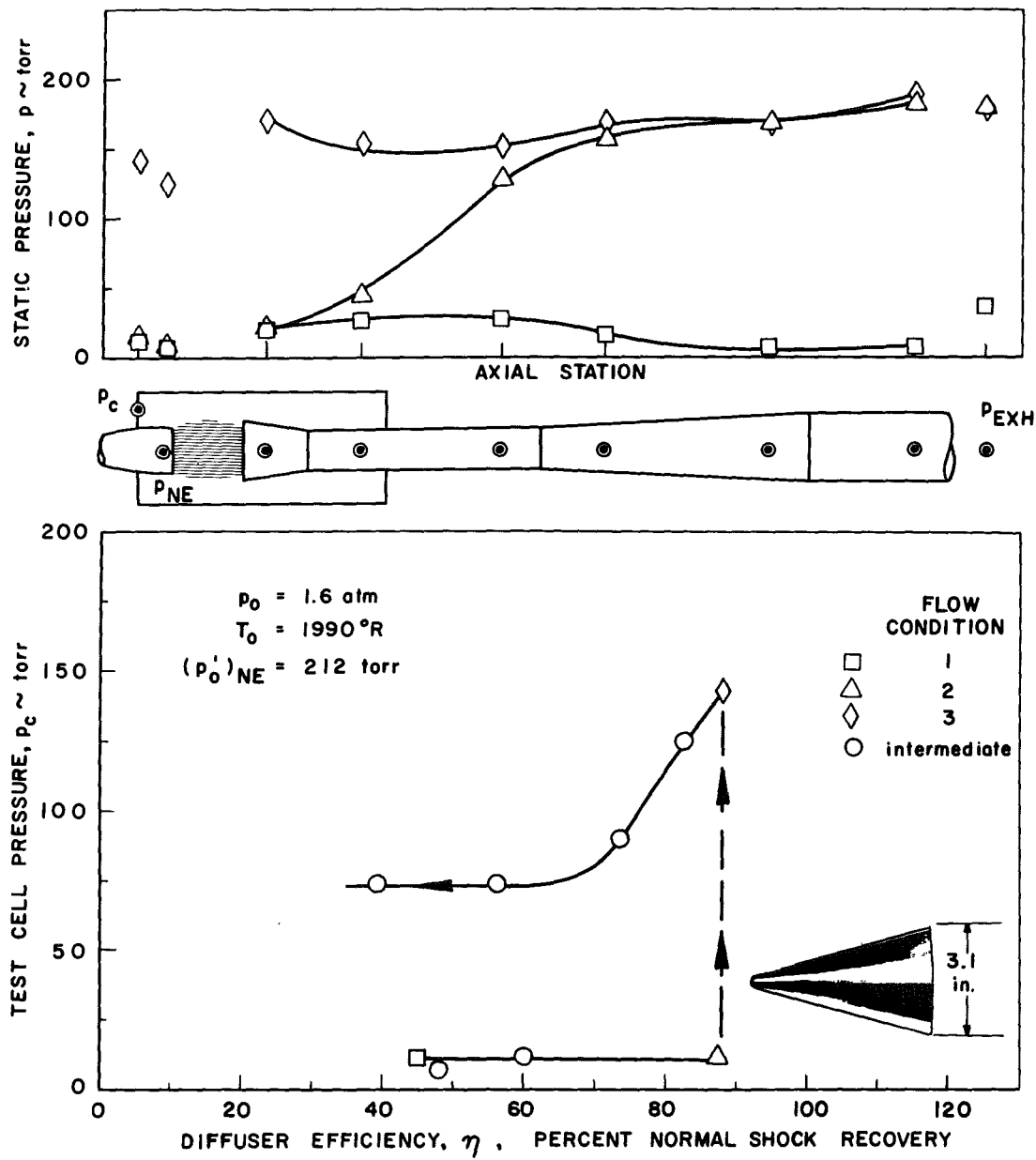
a. Test Section Empty

Fig. 12 Diffuser Efficiencies and Static Pressure Distributions,
 $M_\infty = 3.6$, 10-in. Inlet



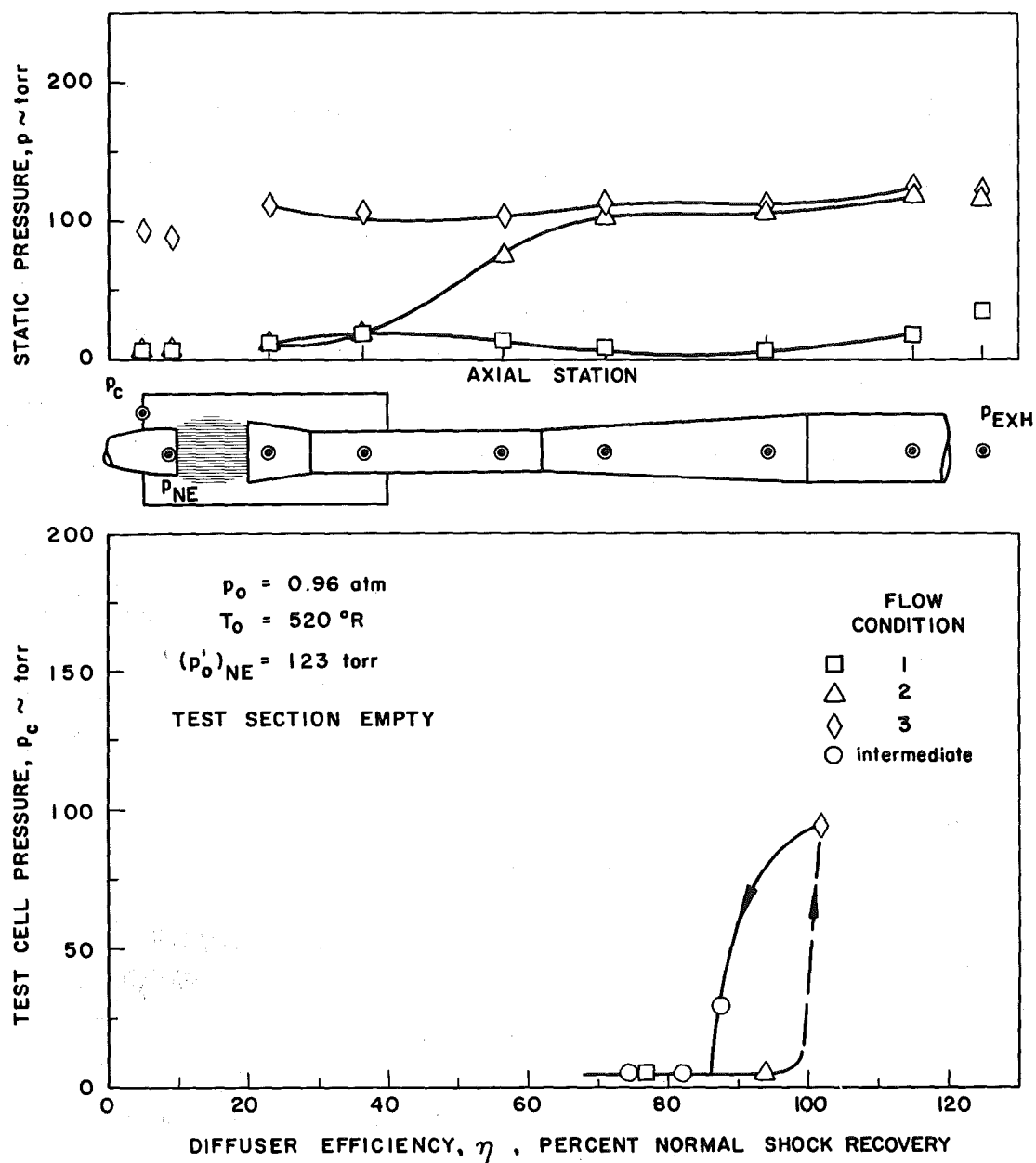
b. 2.0-in. Cone Model

Fig. 12 Continued



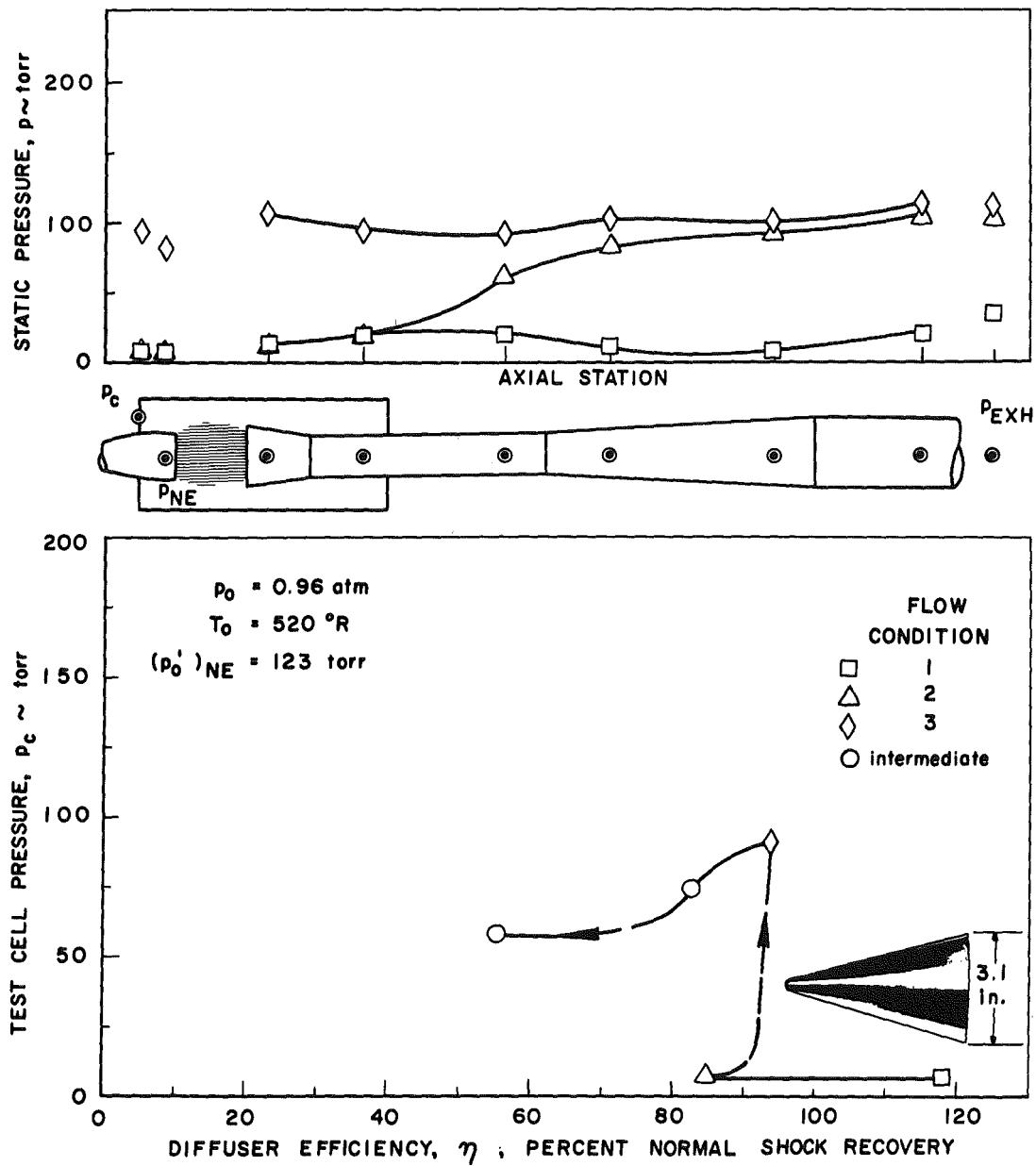
c. 3.1-in. Cone Model

Fig. 12 Concluded



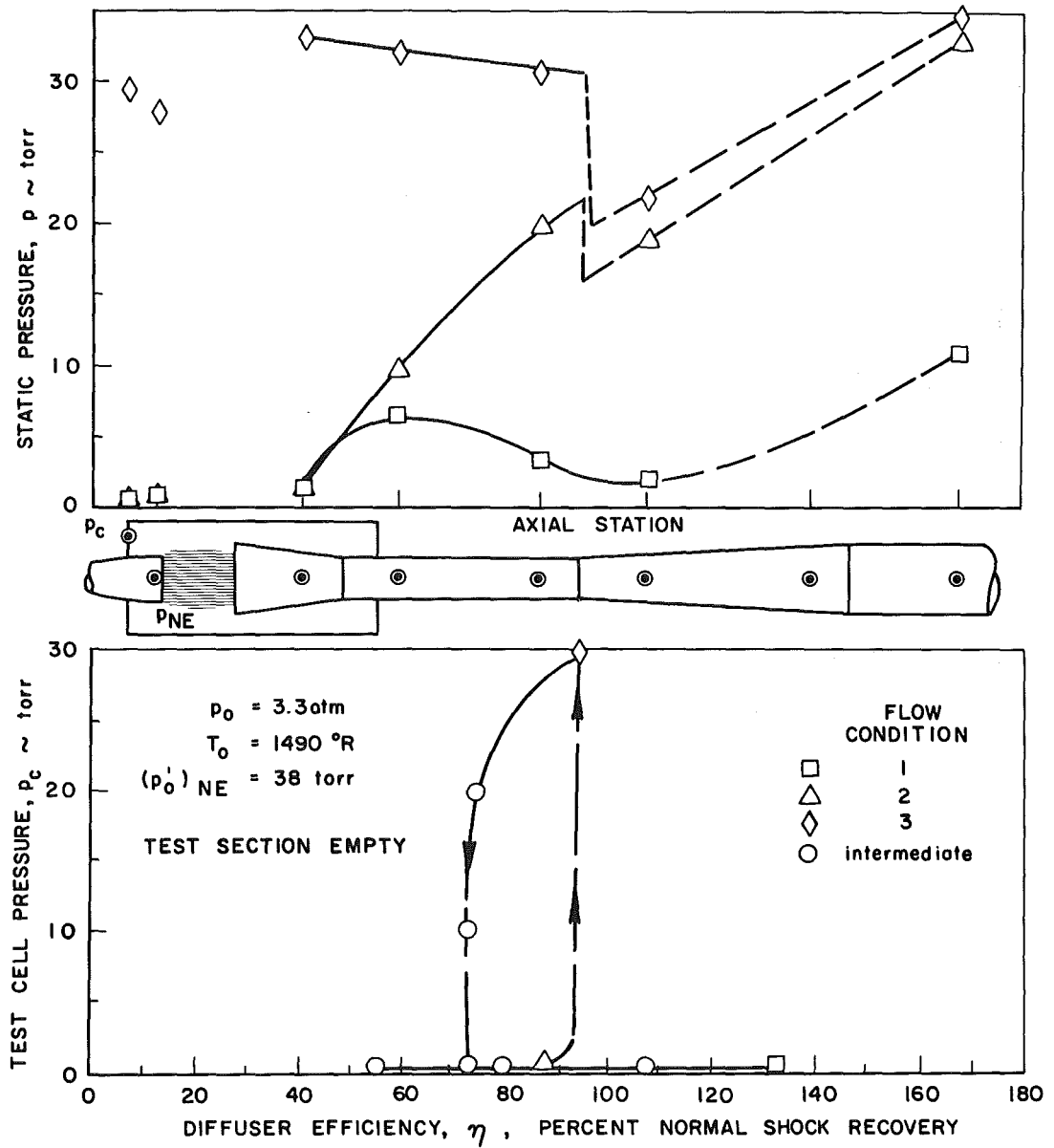
a. Test Section Empty

Fig. 13 Diffuser Efficiencies and Static Pressure Distributions,
 $M_\infty = 3.6$, 10-in. Inlet, Cold Flow



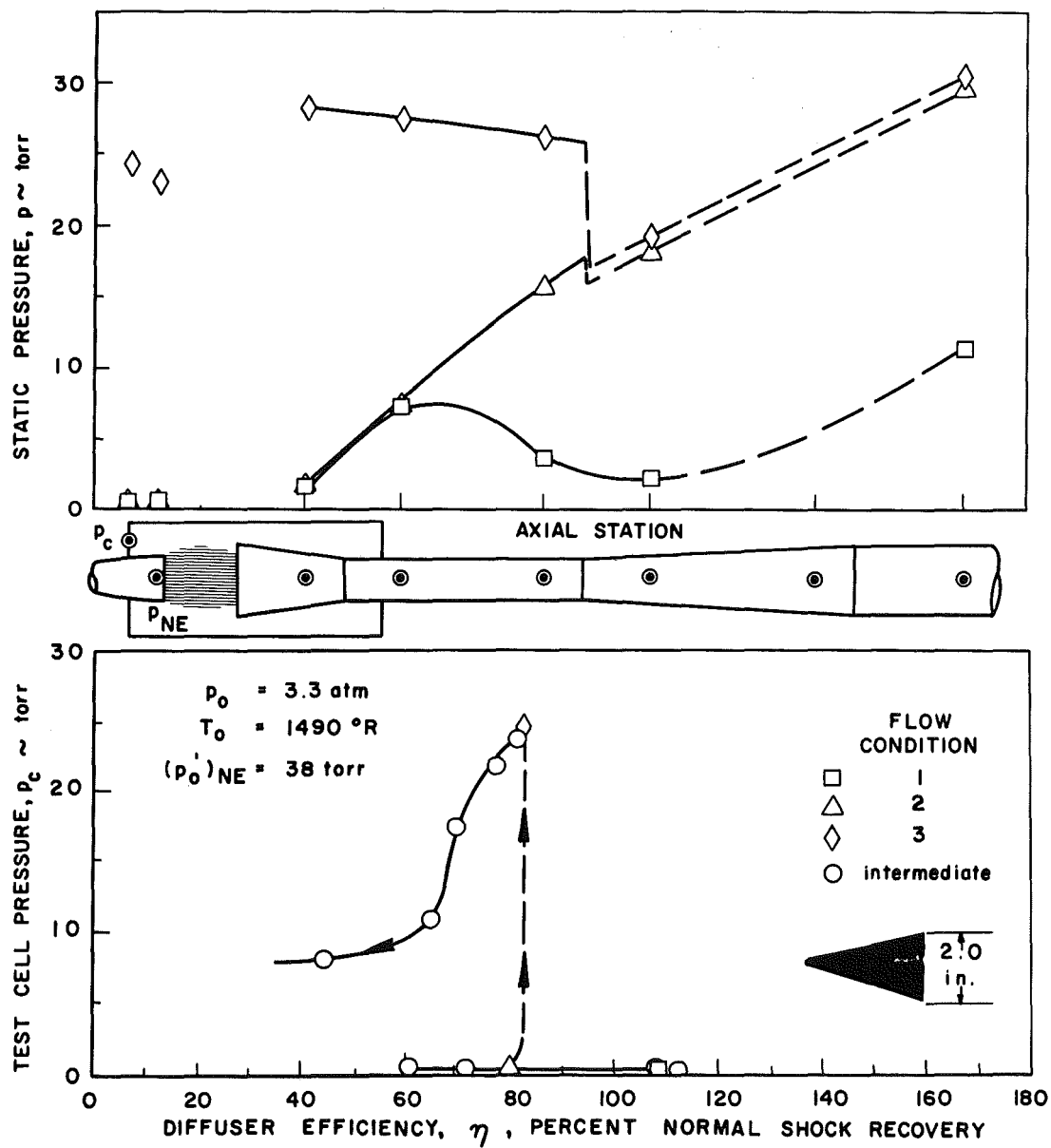
b. 3.1-in. Cone Model

Fig. 13 Concluded



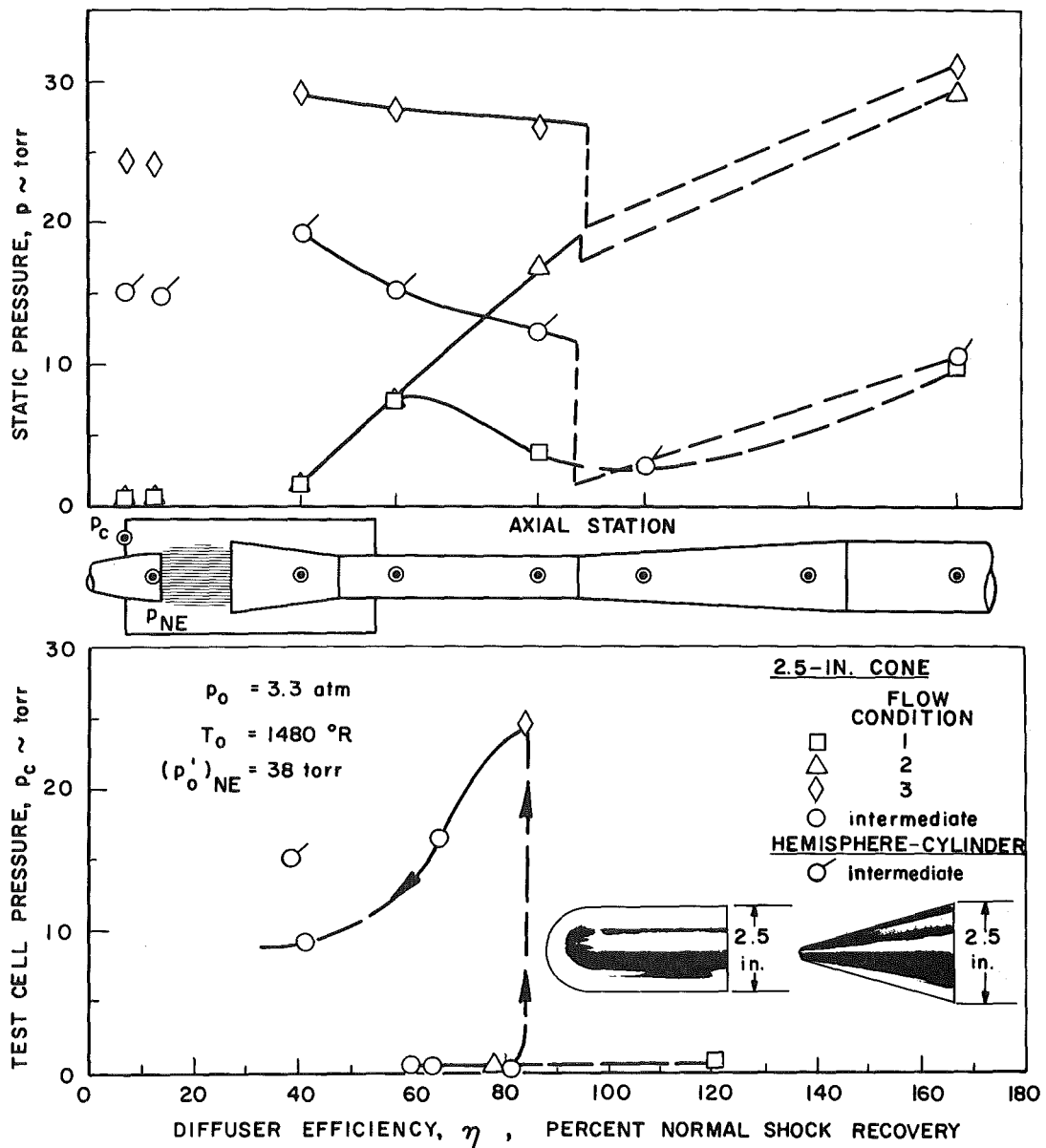
a. Test Section Empty

Fig. 14 Diffuser Efficiencies and Static Pressure Distributions,
 $M_\infty = 7.0$, 12-in. Inlet



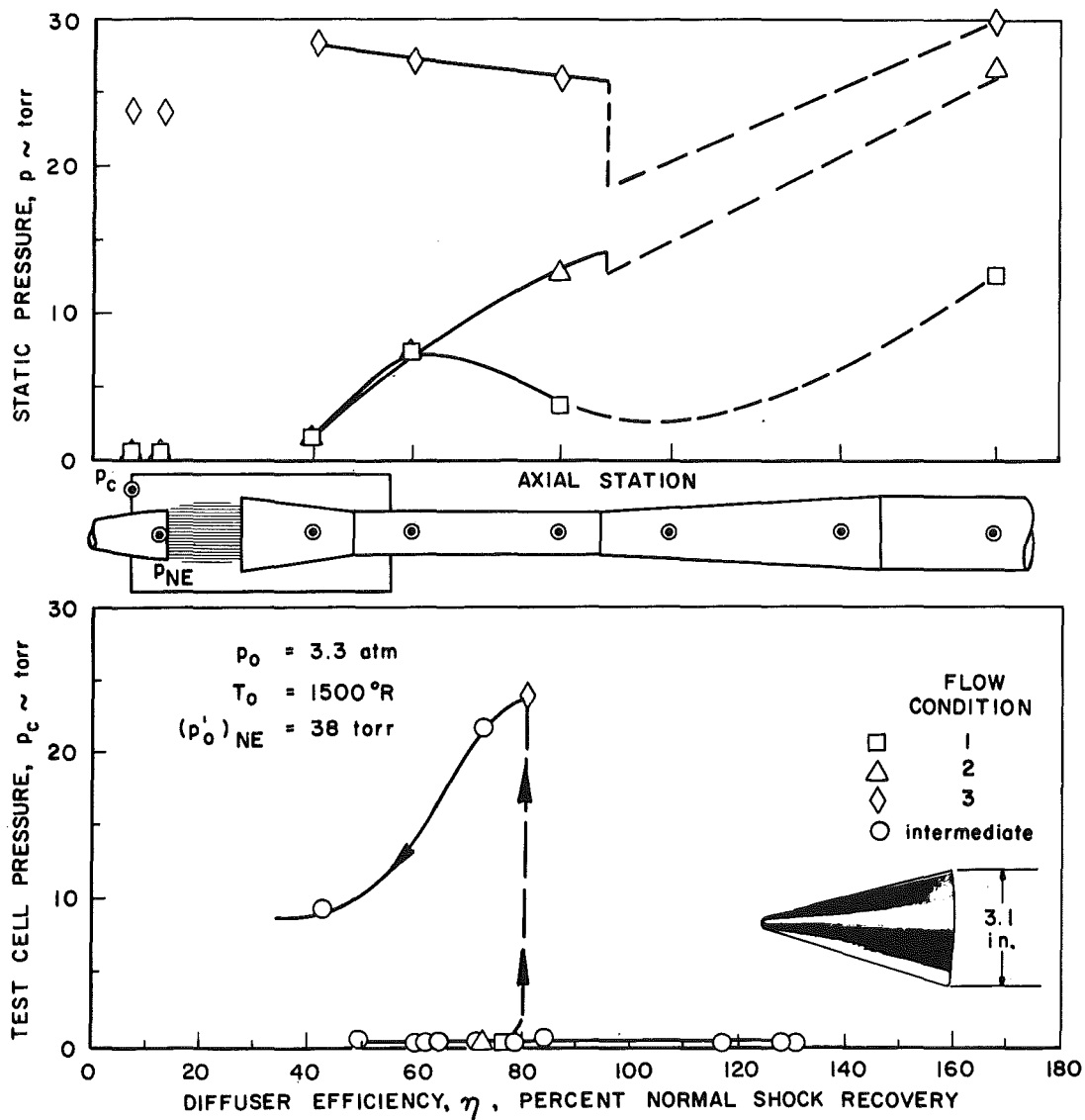
b. 2.0-in. Cone Model

Fig. 14 Continued



c. 2.5-in. Cone and Hemisphere-Cylinder Models

Fig. 14 Continued



d. 3.1-in. Cone Model

Fig. 14 Concluded

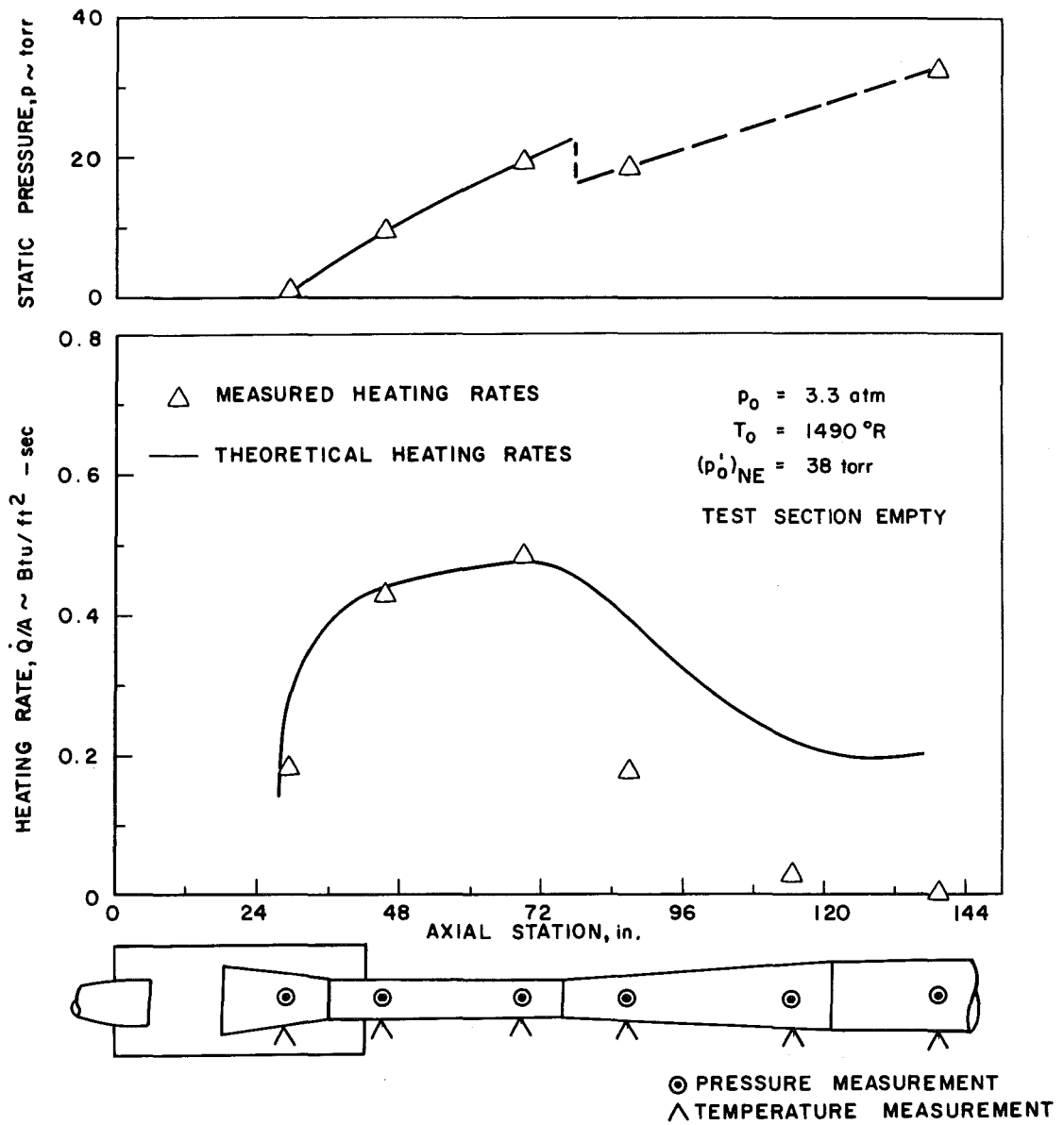


Fig. 15 Diffuser Heating Rate and Static Pressure Distributions,
 $M_\infty = 7.0$, 12-in. Inlet

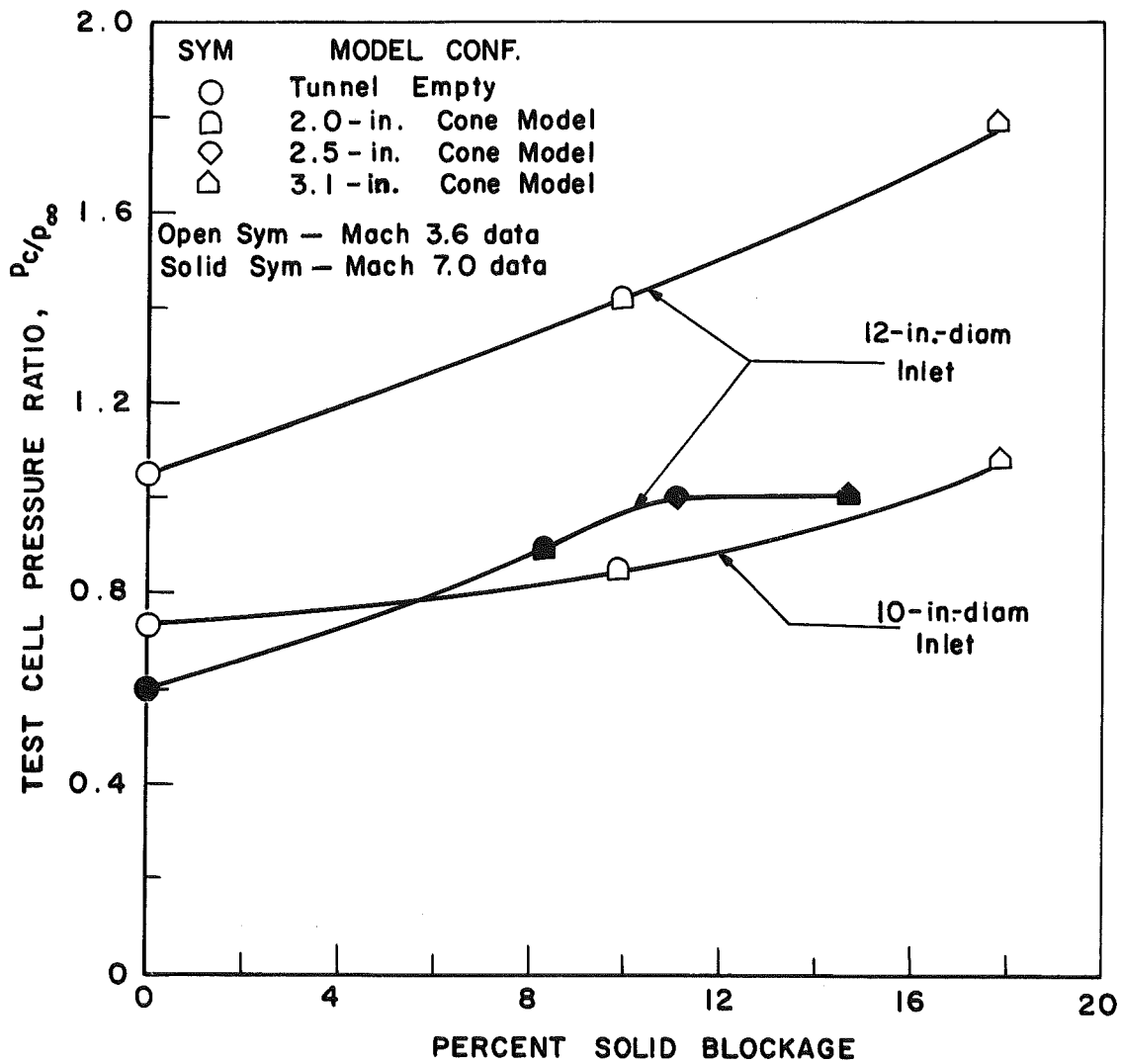


Fig. 16 Model Blockage Effects on Test Cell Pressure, $M_\infty = 3.6$ and 7.0

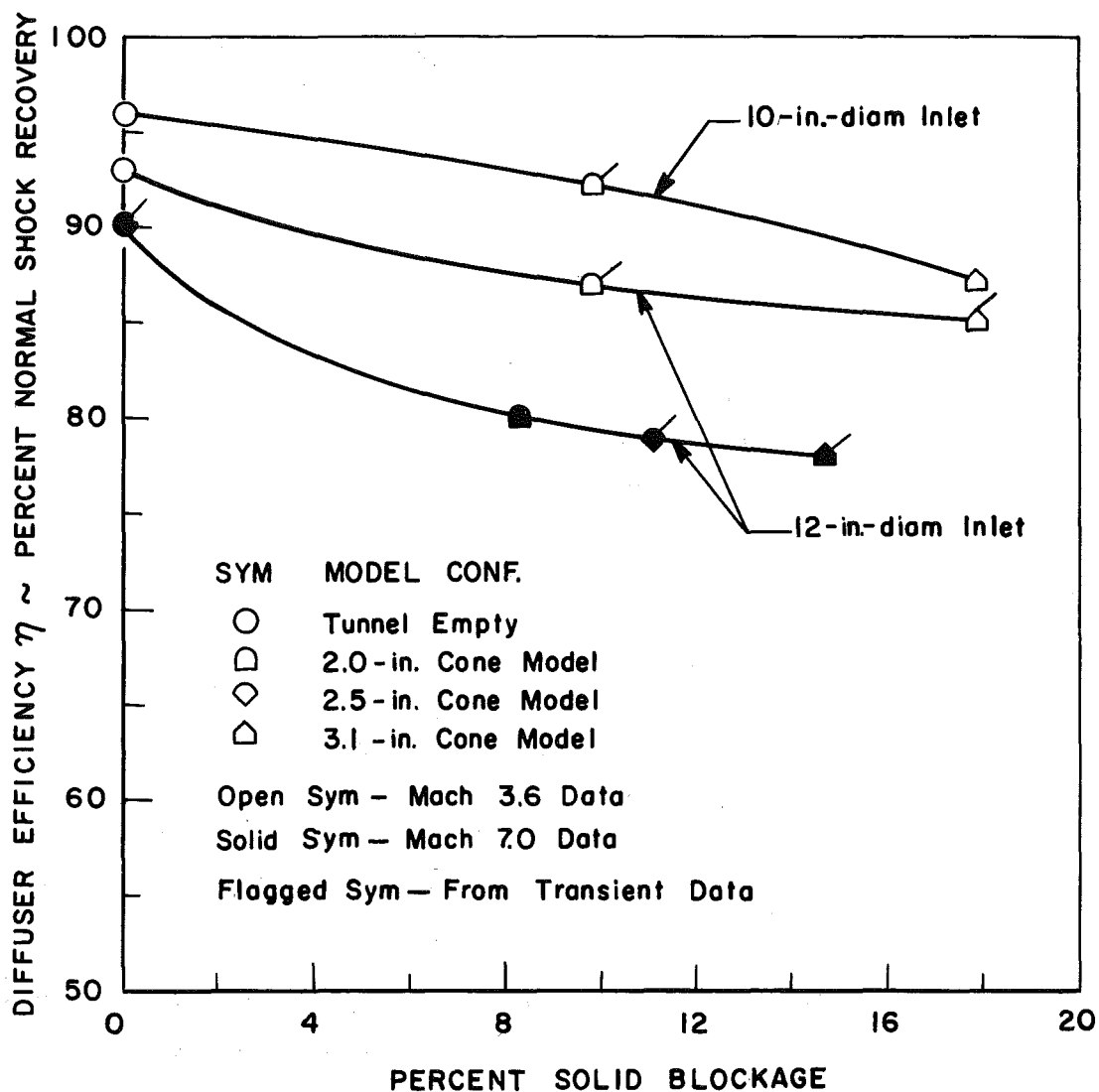


Fig. 17 Model Blockage Effects on Optimum Diffuser Efficiency,
 $M_{\infty} = 3.6$ and 7.0

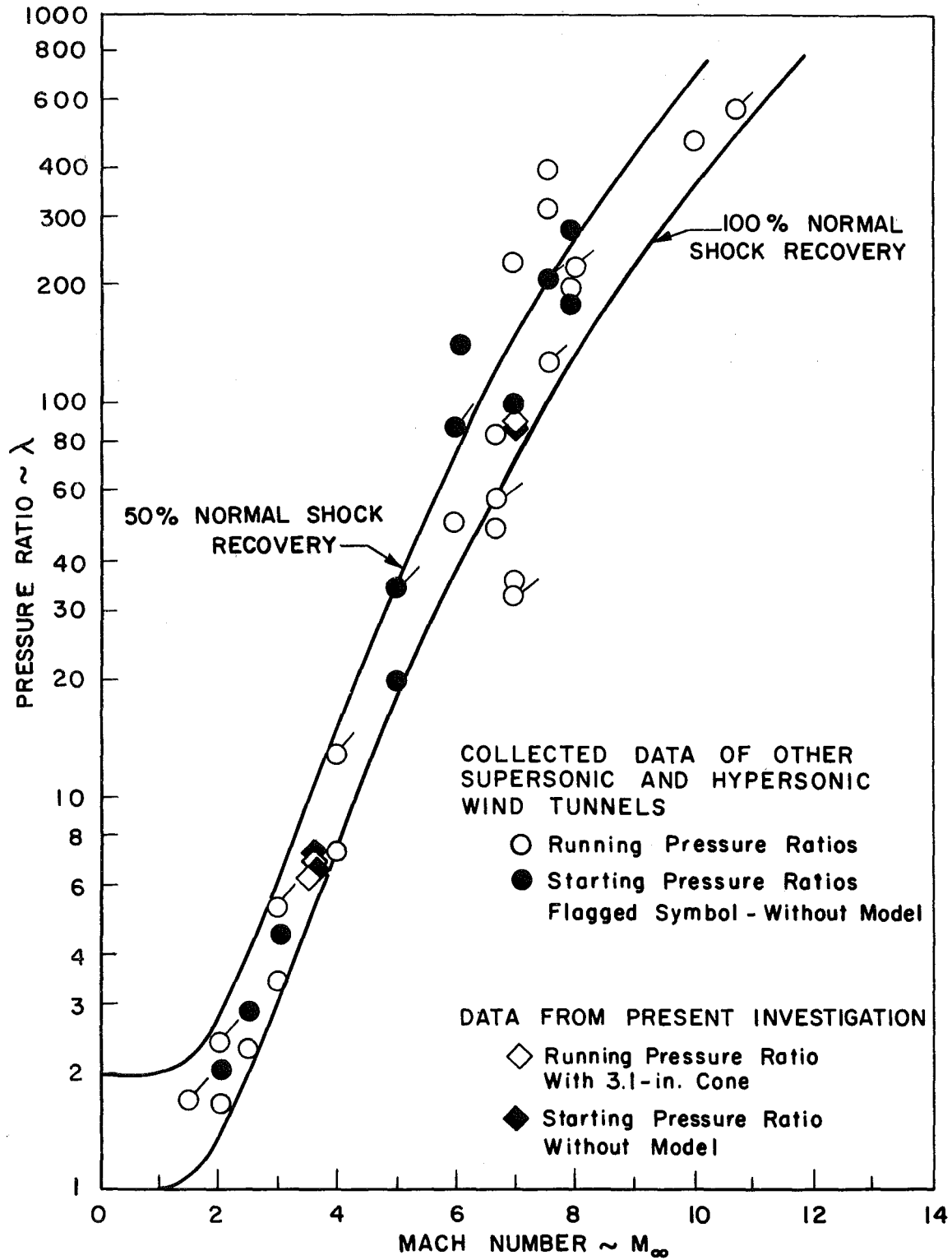


Fig. 18 Comparison of Supersonic and Hypersonic Wind Tunnel Pressure Ratios

DOCUMENT CONTROL DATA - R&D

(Security classification of title, body of abstract and indexing annotation must be entered when the overall report is classified)

1. ORIGINATING ACTIVITY (Corporate author) Arnold Engineering Development Center, ARO, Inc., Operating Contractor, Arnold Air Force Station, Tennessee		2a. REPORT SECURITY CLASSIFICATION UNCLASSIFIED
		2b. GROUP N/A
3. REPORT TITLE AN OPEN-JET WIND TUNNEL INVESTIGATION OF A FIXED-GEOMETRY DIFFUSER SYSTEM AT MACH NUMBERS 3.6 AND 7.0		
4. DESCRIPTIVE NOTES (Type of report and inclusive dates) N/A		
5. AUTHOR(S) (Last name, first name, initial) Austin, Richard F., ARO, Inc.		
6. REPORT DATE March 1966	7a. TOTAL NO. OF PAGES 46	7b. NO. OF REFS 7
8a. CONTRACT OR GRANT NO. AF40(600)1200 b. PROJECT NO. 7778 c. Program Element 62410034 d. Task 777805	9a. ORIGINATOR'S REPORT NUMBER(S) AEDC-TR-66-11 9b. OTHER REPORT NO(S) (Any other numbers that may be assigned this report) N/A	
10. AVAILABILITY/LIMITATION NOTICES Qualified requesters may obtain copies of this report from DDC, and release to foreign governments or foreign nationals must have prior approval of AEDC.		
11. SUPPLEMENTARY NOTES N/A	12. SPONSORING MILITARY ACTIVITY Arnold Engineering Development Center, Air Force Systems Command, Arnold Air Force Station, Tennessee	
13. ABSTRACT A fixed-geometry second-throat diffuser system was tested in an open-jet wind tunnel at Mach numbers 3.6 and 7.0. These tests were conducted at Reynolds numbers of 1×10^6 and 2×10^5 , based on expan- sion nozzle exit diameter. The investigation was conducted to pro- vide diffuser design criteria for the AEDC proposed Hypersonic True Temperature Tunnel (Tripltee). At $M_\infty = 3.6$, empty test section dif- fuser efficiencies of 96 percent of normal shock recovery were achieved. Under similar conditions at $M_\infty = 7.0$, efficiencies of 90 percent were obtained, thus establishing that reasonable diffuser efficiencies can be obtained at both Mach numbers with a single dif- fuser system. Tunnel operation was possible with conical models of up to 18-percent blockage, but diffuser efficiency was reduced by 8 to 12 percent. Tunnel flow could not be established with models in the test section. Models of 8- to 10-percent blockage would not per- mit establishment of tunnel flow at either $M_\infty = 3.6$ or 7.0. It was necessary to inject the models into the flow after the tunnel was started. Limited diffuser heating rate data was obtained at $M_\infty = 7.0$.		

14. KEY WORDS	LINK A		LINK B		LINK C	
	ROLE	WT	ROLE	WT	ROLE	WT
Tripltee						
diffusers						
fixed geometry						
open-jet						
performance						
supersonic flow						
hypersonic flow						
wind tunnel models						
blunt cones						
hemisphere-cylinders						

INSTRUCTIONS

1. ORIGINATING ACTIVITY: Enter the name and address of the contractor, subcontractor, grantee, Department of Defense activity or other organization (*corporate author*) issuing the report.

2a. REPORT SECURITY CLASSIFICATION: Enter the overall security classification of the report. Indicate whether "Restricted Data" is included. Marking is to be in accordance with appropriate security regulations.

2b. GROUP: Automatic downgrading is specified in DoD Directive 5200.10 and Armed Forces Industrial Manual. Enter the group number. Also, when applicable, show that optional markings have been used for Group 3 and Group 4 as authorized.

3. REPORT TITLE: Enter the complete report title in all capital letters. Titles in all cases should be unclassified. If a meaningful title cannot be selected without classification, show title classification in all capitals in parenthesis immediately following the title.

4. DESCRIPTIVE NOTES: If appropriate, enter the type of report, e.g., interim, progress, summary, annual, or final. Give the inclusive dates when a specific reporting period is covered.

5. AUTHOR(S): Enter the name(s) of author(s) as shown on or in the report. Enter last name, first name, middle initial. If military, show rank and branch of service. The name of the principal author is an absolute minimum requirement.

6. REPORT DATE: Enter the date of the report as day, month, year; or month, year. If more than one date appears on the report, use date of publication.

7a. TOTAL NUMBER OF PAGES: The total page count should follow normal pagination procedures, i.e., enter the number of pages containing information.

7b. NUMBER OF REFERENCES: Enter the total number of references cited in the report.

8a. CONTRACT OR GRANT NUMBER: If appropriate, enter the applicable number of the contract or grant under which the report was written.

8b, 8c, & 8d. PROJECT NUMBER: Enter the appropriate military department identification, such as project number, subproject number, system numbers, task number, etc.

9a. ORIGINATOR'S REPORT NUMBER(S): Enter the official report number by which the document will be identified and controlled by the originating activity. This number must be unique to this report.

9b. OTHER REPORT NUMBER(S): If the report has been assigned any other report numbers (*either by the originator or by the sponsor*), also enter this number(s).

10. AVAILABILITY/LIMITATION NOTICES: Enter any limitations on further dissemination of the report, other than those

imposed by security classification, using **standard statements** such as:

- (1) "Qualified requesters may obtain copies of this report from DDC."
- (2) "Foreign announcement and dissemination of this report by DDC is not authorized."
- (3) "U. S. Government agencies may obtain copies of this report directly from DDC. Other qualified DDC users shall request through _____."
- (4) "U. S. military agencies may obtain copies of this report directly from DDC. Other qualified users shall request through _____."
- (5) "All distribution of this report is controlled. Qualified DDC users shall request through _____."

If the report has been furnished to the Office of Technical Services, Department of Commerce, for sale to the public, indicate this fact and enter the price, if known.

11. SUPPLEMENTARY NOTES: Use for additional explanatory notes.

12. SPONSORING MILITARY ACTIVITY: Enter the name of the departmental project office or laboratory sponsoring (*paying for*) the research and development. Include address.

13. ABSTRACT: Enter an abstract giving a brief and factual summary of the document indicative of the report, even though it may also appear elsewhere in the body of the technical report. If additional space is required, a continuation sheet shall be attached.

It is highly desirable that the abstract of classified reports be unclassified. Each paragraph of the abstract shall end with an indication of the military security classification of the information in the paragraph, represented as (TS), (S), (C), or (U).

There is no limitation on the length of the abstract. However, the suggested length is from 150 to 225 words.

14. KEY WORDS: Key words are technically meaningful terms or short phrases that characterize a report and may be used as index entries for cataloging the report. Key words must be selected so that no security classification is required. Identifiers, such as equipment model designation, trade name, military project code name, geographic location, may be used as key words but will be followed by an indication of technical context. The assignment of links, rules, and weights is optional.